Journal of High Speed Networks 16 (2007) 353–377
IOS Press 

# Network profit optimization for traffic grooming in WDM networks with wavelength converters

James Yiming Zhang [a], Jing Wu [b,*], Oliver Yang [a] and Michel Savoie [b]
[a] *School of Information Technology and Engineering, University of Ottawa, Ottawa, ON, K1N 6N5, Canada*
*E-mail: {yizhang, yang}@site.uottawa.ca*
[b] *Communications Research Centre Canada, Ottawa, ON, K2H 8S2, Canada*
*E-mail: {jing.wu, michel.savoie}@crc.ca*

**Abstract.** The traffic grooming technique provides a two-layer traffic engineering capability by aggregating and routing up-layer low-bandwidth traffic flows over low-layer re-configurable routed high-bandwidth connections. In this paper, we optimize traffic grooming for static traffic in mesh Wavelength Division Multiplexing (WDM) networks with wavelength converters. The optimization objective is to maximize network profit, which is the difference between resource cost and the revenue generated (by selecting profitable traffic flows). A constrained integer linear programming formulation is given, and a decomposition using Lagrangian relaxation is proposed. We then present a systematic approach to solve this problem and to obtain a performance bound for an arbitrary topology mesh network. Our approach can select traffic flows based on their profit, while obtaining their data path routing, lightpath routing and wavelength assignment at the same time. Our performance evaluation also reveals the impact of various cost parameters on the profit objective.

Keywords: WDM networks, traffic grooming, routing and wavelength assignment, network profit optimization, Lagrangian relaxation, wavelength conversion

## 1. Introduction

Wavelength routing in Wavelength Division Multiplexing (WDM) networks enables the re-configuration of virtual topologies of optical networks, and provides an opportunity for joint two-layer traffic engineering [1–4]. Lightpaths are routed in a WDM network and each of them is assigned to a wavelength channel on a link. Since wavelength converters may be used, a lightpath may use different wavelengths on different links. At the entry of a lightpath, electrical domain traffic flows are aggregated (i.e., groomed) together and carried by the lightpath. In this paper, we simply refer to the electrical domain traffic flows as traffic flows. At the intermediate nodes of a lightpath, the traffic flows pass through optical switches without electrical processing. At the exit of a lightpath, the individual traffic flows are restored to their electrical form. If a traffic flow has not yet reached its final destination, it is groomed with other traffic flows and carried by another lightpath. We refer the traffic grooming type discussed herein as multi-hop traffic grooming [5], where the lightpath bandwidth is shared by traffic flows between different source-destination pairs. The multi-hop traffic grooming problem is an extension of the virtual topology design problem of a WDM network. It is a joint design issue of two layers of traffic engineering: the routing of lightpaths over fibres, and the routing of traffic flows over lightpaths. This traffic grooming problem and the associated cross-layer cost minimization aspects have not been addressed in most of the virtual topology design studies (e.g., see survey [2]).

*Corresponding author: Jing Wu, Communications Research Centre Canada, Ottawa, ON, K2H 8S2, Canada. Tel.: +1 613 998 2474; Fax: +1 613 990-8382; E-mail: jing.wu@crc.ca.

Traffic grooming research has two flavours: static and dynamic. Depending on whether the arrival and departure time of traffic flows are random or are known in advance, traffic grooming is classified as dynamic (e.g., [5,10]) and static (e.g., [6–9]), respectively. In this paper, we study the static traffic grooming.

For the static traffic grooming problem, how to select profitable traffic flows is an untouched problem. Assuming that all the traffic flows should be accepted, most previous studies aim at minimizing costs [2,9,17]. This assumption is not practical: the revenue generated by some traffic flows may not recover their provisioning costs, because no efficient provisioning scheme exists for them. A few previous studies dealt with the throughput maximization or revenue optimization problems [8,18,19], by using throughput maximization to prioritize the traffic flows based on their efficiency of resource utilization. Unfortunately, the efficiency of traffic grooming and lightpath provisioning schemes is implicitly evaluated without modelling the cost. Therefore, it is unknown whether providing service to a traffic flow is profitable or not. The revenue optimization is a variation of throughput maximization. For a given network, the revenue maximization leads to maximal profit. The revenue was modelled as a weighted throughput [8] or modelled based on service differentiation for lightpath protection [18], but the cost parameters were not modelled, and their impact on the profit was not studied. While maximizing throughput and minimizing the number of lightpaths were modelled in [19] as two competing objectives and were jointly optimized using the multi-objective optimization technique, the relationship of these two objectives to the profit was not revealed. In this paper, we study the static traffic grooming in WDM networks with wavelength converters. Different from the previous studies, both the cost minimization and throughput maximization are incorporated into our profit optimization. We propose a model for profit optimization for static traffic grooming in WDM networks. The profit is modelled as the difference between resource costs and the revenue generated by accepted traffic flows. Our model can identify profitable traffic flows and examine the impact of cost parameters on the profit objective.

Different topologies are studied in the traffic grooming problem. Due to its simplicity, the ring topology is used in most previous research [9,11,12]. However, with its superior efficiency, the mesh topology is increasingly used. Traffic grooming in the mesh topology is challenging and is reported in only a few recent publications [6–8,13–15]. But, the lightpath routing problem was neglected in [13,15]. In [8], heuristic algorithms were proposed without comparing results obtained from the heuristics to the optimal ones. In [7], although a decomposition method was given the objective of minimizing the total number of transponders, it is unclear how the decomposition method applies to other general optimization objectives, and how the solutions of the sub-problems should be coordinated. Our traffic grooming research is conducted on a mesh network topology. Following our previous study on the traffic grooming problem for SONET-over-WDM networks [16], we extend the research by providing a modified optimization objective, proof of the performance bound, modified heuristics, and new optimization results.

Existing optimization methods for the static traffic grooming problem in the mesh topology suffer from high computational complexity. Thus they are not applicable to practical networks. This problem can be formulated as a constrained Integer Linear Programming (ILP) problem [2,7,8,14]. It has been proved that this problem is Non-Polynomial (NP) complete [12]. For practical networks, this problem cannot be solved by using an ILP solver software such as CPLEX. For example, even for a small network consisting of 6 nodes and 8 links in [8], their CPLEX approach could not compute the optimal solution within a reasonable time, and the computation was terminated before reaching the optimal solution. It is not uncommon to find only heuristics to solve the ILP problem [6–8,14] for practical networks. In our study, we apply the Lagrangian Relaxation (LR) and subgradient methods to this problem. We can achieve a feasible solution for fairly large networks: each traffic flow is identified as profitable or not, and profitable traffic flows are provided with optimized provisioning schemes. In addition, a performance bound is obtained to evaluate the optimality of the solution.

In summary, the contributions of this paper are:

– Formulating the network profit optimization problem for static traffic grooming in WDM networks with wavelength converters;
– Providing a generic network model for the use of a limited number of wavelength converters at selected nodes. Our model can be applied to networks without wavelength converters or with an unlimited number of wavelength converters as a special case. Hence, our model can be used to study cases of a complete range of wavelength converter;

– Proposing an LR-based method to solve the optimization problem. The method has less computational complexity than the existing methods. Thus, it is applicable to practical networks;
– Providing a framework to obtain performance bounds for the static traffic grooming in arbitrary topology networks;
– Demonstrating the effectiveness of the proposed method for two large networks with 32 wavelengths and 14 or 22 nodes;
– Revealing different behaviours of various bandwidth traffic flows, via quantitative optimized results, as the cost of electrical layer grooming increases;
– Examining the contribution of wavelength converters to the profit objective for static traffic patterns.

This paper is organized as follows: in Section 2, the network profit optimization problem is formulated. A solution to the profit model is proposed based on the LR and subgradient methods in Section 3. The numeric results are presented in Section 4, followed by the conclusions in Section 5.

## 2. Formulation of the network profit optimization problem

To formulate our profit optimization problem, we establish the following design variables of our model:

– Admission status of each traffic flow, i.e., the selection of profitable traffic flows.
– Routing of traffic flow over lightpaths, i.e., which lightpaths are used to carry each accepted traffic flow. This subset of design variables represents a static single layer routing problem.
– Lightpath setup status between each node pair, i.e., which lightpaths should be set up. Setting up multiple lightpaths between a node pair is allowed. Such lightpaths may or may not take the same route. If such lightpaths choose the same route, they must use different wavelength channels on common fibres.
– Lightpath routing over fibres, i.e., which fibres does each lightpath travel through.
– Wavelength assignment for lightpaths, i.e., which wavelength channel is used on each fibre. In this paper, since wavelength converters are allowed, a lightpath may take different wavelength channels on different links.
– Assignment schemes of wavelength converters to lightpaths, i.e., which lightpath uses which wavelength converter at which node. The last four subsets of design variables form a classical Routing and Wavelength Assignment (RWA) problem.

The above design variables are not completely independent. For example, the selection of profitable traffic flows depends on how lightpaths are set up and how traffic flows are routed over the lightpaths. The assignment schemes of wavelength converters to lightpaths also depend on the wavelength assignment for lightpaths.

We formulate the objective function as follows:

$$\max(f), \quad \text{where } f = \sum_{(p,q)} \sum_{0<z\leqslant Z_{pq}} \gamma_{pqz} P_{pqz} G_{pqz} - \sum_{(p,q)} \sum_{0<z\leqslant Z_{pq}} E_{pqz} - \sum_{(s,d)} \sum_{0<n\leqslant N_{sd}} D_{sdn}. \tag{1}$$

The profit objective is composed of three parts: the revenue generated by accepted traffic flows, the traffic grooming cost, and the lightpath cost. We adopt a virtual unit proportional to the dollar unit for the cost, the revenue and the profit. It is assumed that the traffic matrix and the expected revenue for each traffic flow are given. We denote $\chi_{pqz}$ as the $z$th traffic flow between the node pair $(p, q)$, and denote $Z_{pq}$ as the maximum number of traffic flows between the node pair $(p, q)$. The revenue coefficient for accepting the traffic flow $\chi_{pqz}$ is $P_{pqz}$, measured by the service charge per bandwidth unit. For simplicity, we use multiples of the equivalent bandwidth of an STS-1 (Synchronous Transport Signal of level One) channel as a basic bandwidth unit. The bandwidth requirement of $\chi_{pqz}$ is $G_{pqz}$. The admission status of $\chi_{pqz}$ is $\gamma_{pqz}$, which equals one if $\chi_{pqz}$ is determined to be profitable and, therefore, accepted; or zero otherwise. The electrical domain traffic grooming cost for $\chi_{pqz}$ is $E_{pqz}$. We model the traffic grooming cost $\chi_{pqz}$ as the total cost of the electrical domain grooming cost for $\chi_{pqz}$ before $\chi_{pqz}$ is carried by a lightpath.

$$E_{pqz} = \sum_{(s,d)} \sum_{0<n\leqslant N_{sd}} \upsilon_{sdn}^{pqz} V_{pqz} \quad \text{for all traffic flows } \chi_{pqz}. \tag{2}$$

The routing status of $\chi_{pqz}$ over lightpath $s_{sdn}$ is denoted by $\upsilon_{sdn}^{pqz}$, which equals one when $\chi_{pqz}$ is routed through the lightpath $s_{sdn}$, or zero otherwise. We denote the $n$th lightpath between the node pair $(s, d)$ as $s_{sdn}$. The coefficient for the traffic grooming cost is $V_{pqz}$. Each traffic flow is groomed before it is carried by a lightpath. In our model, the electrical processing at the end of a lightpath is not counted. Thus, a traffic flow using a single hop lightpath has one-time traffic grooming cost; a traffic flow using two lightpath hops has two-time traffic grooming cost, and so on.

The routing cost for lightpath $s_{sdn}$ is $D_{sdn}$. The maximum number of lightpaths between node pair $(s, d)$ is denoted by $N_{sd}$. We model the lightpath cost as the sum of the transmitter cost, the receiver cost, and the total cost of all the wavelength channels that the lightpath uses.

$$D_{sdn} = \alpha_{sdn}(t_s + r_d) + \sum_{(i,j)} \sum_{0<c\leqslant W} \delta_{ijc}^{sdn} d_{ijc} + \sum_{j} \phi_j^{sdn} c_j \quad \text{for all lightpaths } s_{sdn}. \tag{3}$$

The setup status of $s_{sdn}$ is denoted by $\alpha_{sdn}$, which equals one when $s_{sdn}$ is set up; or zero otherwise. The cost of a transmitter at source node $s$ is $t_s$. The cost of a receiver at destination node $d$ is $r_d$. The usage of the wavelength channel $w_{ijc}$ (i.e., the $c$th wavelength channel between node pair $(i, j)$) by $s_{sdn}$ is denoted by $\delta_{ijc}^{sdn}$, which equals one when $s_{sdn}$ travels through $w_{ijc}$; or zero otherwise. The wavelength channel count on a fibre is denoted by $W$. The cost of $w_{ijc}$ is $d_{ijc}$. The usage of a wavelength converter by $s_{sdn}$ at an intermediate node $j$ is denoted by $\phi_j^{sdn}$, which equals one when a wavelength converter is used; or zero otherwise. The cost of a wavelength converter at an intermediate node $j$ is $c_j$.

The constraints are organized in three categories: the dependence of the electrical and optical domains (i.e., constraint (4)), pure electrical domain constraint (i.e., constraint (5)), and pure optical domain constraints (i.e., constraints (6)–(11)).

(a) Lightpath bandwidth constraint, i.e., the total bandwidth of traffic flows being routed over a lightpath should be less than the lightpath bandwidth $C$. In this paper, we assume that the lightpath bandwidth $C$ has 48 bandwidth units.

$$\sum_{(p,q)} \sum_{0<z\leqslant Z_{pq}} \upsilon_{sdn}^{pqz} G_{pqz} \leqslant C\alpha_{sdn} \quad \text{for all lightpaths } s_{sdn}. \tag{4}$$

(b) Traffic flow continuity constraint, i.e., every accepted traffic flow continues from its source to destination.

$$\sum_{d} \sum_{0<n\leqslant N_{sd}} \upsilon_{sdn}^{pqz} - \sum_{d} \sum_{0<n\leqslant N_{ds}} \upsilon_{dsn}^{pqz} = \begin{cases} \gamma_{pqz} & \text{if } s = p, \\ -\gamma_{pqz} & \text{if } s = q, \\ 0 & \text{otherwise} \end{cases} \quad \text{for all traffic flows } \chi_{pqz}. \tag{5}$$

At the left-hand side of the equation, the first part represents the total number of traffic flows that originate from node $s$, while the second part represents the total number of traffic flows that terminate at node $s$. Unless node $s$ is the source or destination of $\chi_{pqz}$, the incoming and outgoing traffic flows at node $s$ should balance.

(c) Lightpath continuity constraint, i.e., every lightpath continues from its source to destination.

$$\sum_{j}\sum_{0<c\leqslant W}\delta_{ijc}^{sdn}-\sum_{j}\sum_{0<c\leqslant W}\delta_{jic}^{sdn}=\begin{cases}\alpha_{sdn} & \text{if } i=s,\\ -\alpha_{sdn} & \text{if } i=d,\\ 0 & \text{otherwise}\end{cases}\quad \text{for all lightpaths } s_{sdn}. \tag{6}$$

At the left-hand side of the equation, the first part represents the total number of lightpaths that originate from node $i$ (regardless of their wavelength channels), while the second part represents the total number of lightpaths that terminate at node $i$ (also, regardless of their wavelength channels). Unless node $i$ is the source or destination of $s_{sdn}$, the incoming and outgoing traffic flows at node $i$ should balance.

(d) Wavelength conversion constraint, i.e., when a lightpath changes its wavelength at an intermediate node, a wavelength converter must be used.

$$\phi_j^{sdn}=\begin{cases}1, & \exists \text{ an upstream node } m \text{ and a dowstream node } k,\\ & \text{and } b\neq c, \text{ that satify } \delta_{mjb}^{sdn}=\delta_{jkc}^{sdn}=1,\\ 0, & \text{otherwise}\end{cases}\quad \text{for all intermediate nodes } j. \tag{7}$$

(e) Wavelength converter quantity constraint, i.e., the number of used wavelength converters in a given node cannot exceed the number of installed wavelength converters at the same node.

$$\sum_{(s,d)}\sum_{0<n\leqslant N_{sd}}\phi_j^{sdn}\leqslant F_j\quad \text{for all intermediate nodes } j. \tag{8}$$

The number of installed wavelength converters at an intermediate node $j$ is $F_j$. The wavelength converters are installed based on a share-per-node structure, which allows any incoming lightpath to access any available wavelength converter, and allows the output of a wavelength converter to go to any output port of the node.

(f) Wavelength channel exclusive usage constraint, i.e., no more than one lightpath may be routed through any wavelength channel.

$$\sum_{(s,d)}\sum_{0<n\leqslant N_{sd}}\delta_{ijc}^{sdn}\leqslant 1\quad \text{for all wavelength channels } w_{ijc}. \tag{9}$$

(g) Transmitter quantity constraint, i.e., the number of lightpaths originating from a node cannot be more than the number of transmitters at the node. In this paper, we assume that all transmitters operate at any wavelength.

$$\sum_{d}\sum_{0<n\leqslant N_{sd}}\alpha_{sdn}\leqslant T_s\quad \text{for all source nodes } s. \tag{10}$$

The number of transmitters at source node $s$ is $T_s$.

(h) Receiver quantity constraint, i.e., the number of lightpaths terminating at a node cannot be more than the number of receivers at the node. We assume that all receivers operate at any wavelength.

$$\sum_{s}\sum_{0<n\leqslant N_{sd}}\alpha_{sdn}\leqslant R_d\quad \text{for all destination nodes } d. \tag{11}$$

The number of receivers at destination node $d$ is $R_d$.

Using the above notations, the design variables in our model are:

– Traffic flow admission status $\gamma$, where $\gamma = (\gamma_{pqz})$ for all traffic flows $\chi_{pqz}$;
– Traffic flow routing scheme $\upsilon$, where $\upsilon = (\upsilon_{sdn}^{pqz})$ for all traffic flows $\chi_{pqz}$ and all lightpaths $s_{sdn}$;
– Lightpath setup status $\alpha$, where $\alpha = (\alpha_{sdn})$ for all lightpaths $s_{sdn}$;
– Lightpath routing and wavelength assignment scheme $\delta$, where $\delta = (\delta_{ijc}^{sdn})$ for all lightpaths $s_{sdn}$ and all wavelength channels $w_{ijc}$;
– Assignment scheme of wavelength converters to lightpaths, denoted by $\phi$, where $\phi = (\phi_j^{sdn})$ for all lightpaths $s_{sdn}$ and all intermediate nodes $j$.

The objective function $\max_{\gamma,\upsilon,\alpha,\delta,\phi}[f(\gamma, \upsilon, \alpha, \delta, \phi)]$ is to maximize a weighted summation of all design variables. All the design variables are integers of value either 1 or 0. So the problem is a constrained ILP problem.

## 3. Network profit optimization method and analysis

After providing an overview of our solution framework in Section 3.1, we provide an LR-based decomposition of the profit optimization problem in Section 3.2. Solutions of the sub-problems are briefly described in Section 3.3. A subgradient-based method to solve the dual problem is presented in Section 3.4. We highlight the heuristics used to obtain feasible solutions for the primal problem in Section 3.5. The computational complexity of the proposed algorithm is analyzed in Section 3.6.

### *3.1. Overview of the solution framework*

Our optimization method relies on the theoretical groundwork in Section 3.2 for the decomposition into less complex sub-problems. By relaxing selected constraints, and transforming the relaxed constraints into soft "price" terms, we derive a Lagrangian function [20], in which Lagrange multipliers (soft "prices") are used to reflect the relaxed hard constraints. We define a dual function as the supremum of the Lagrangian function. A dual problem is created as minimizing the dual function. During the subgradient-based iterations of solving a dual problem, the optimization process is gradually guided to respect the relaxed constraints. Such iterations have been proved to converge to the optimum (see Section 6.3.1 of [21]). The overall algorithm is an optimization procedure. The heuristic algorithm in the optimization framework serves only as a projection from the dual space (consisting of the variables for the dual problem, i.e., the Lagrangian multipliers) to the primal space (consisting of the design variables for the profit optimization problem). Strictly obeying the relaxed constraints is guaranteed in the projection of an infeasible solution to a feasible solution by a heuristic algorithm. The solution framework is illustrated in Fig. 1.

Our method can solve the optimization problem for practical scale networks. CPLEX is able to obtain the optimal solution of this problem for very small networks, but cannot solve this problem for practical networks. Existing heuristic algorithms cannot obtain a quantitative performance bound. Thus, the performance of heuristics is never checked for any practical network. Our method obtains a performance bound for the profit optimization problem for practical scale networks. We prove that the minimal dual value is an upper bound for the primal function.

There is a duality gap between the minimal dual value (i.e., value for the dual function) and the maximal primal value (i.e., value for the primal function). The maximal primal value represents the best achievable profit. It corresponds to a feasible provisioning scheme. The duality gap indicates the optimality of the solutions. A good near-optimal solution leads to a small duality gap.

### *3.2. Decomposition of the profit optimization problem*

We relax selected constraints to derive a Lagrangian function, and decompose the profit optimization problem into sub-problems. The constraints that we choose to relax are the lightpath bandwidth constraint (4), the wavelength converter quantity constraint (8), the wavelength channel exclusive usage constraint (9), and the transmitter

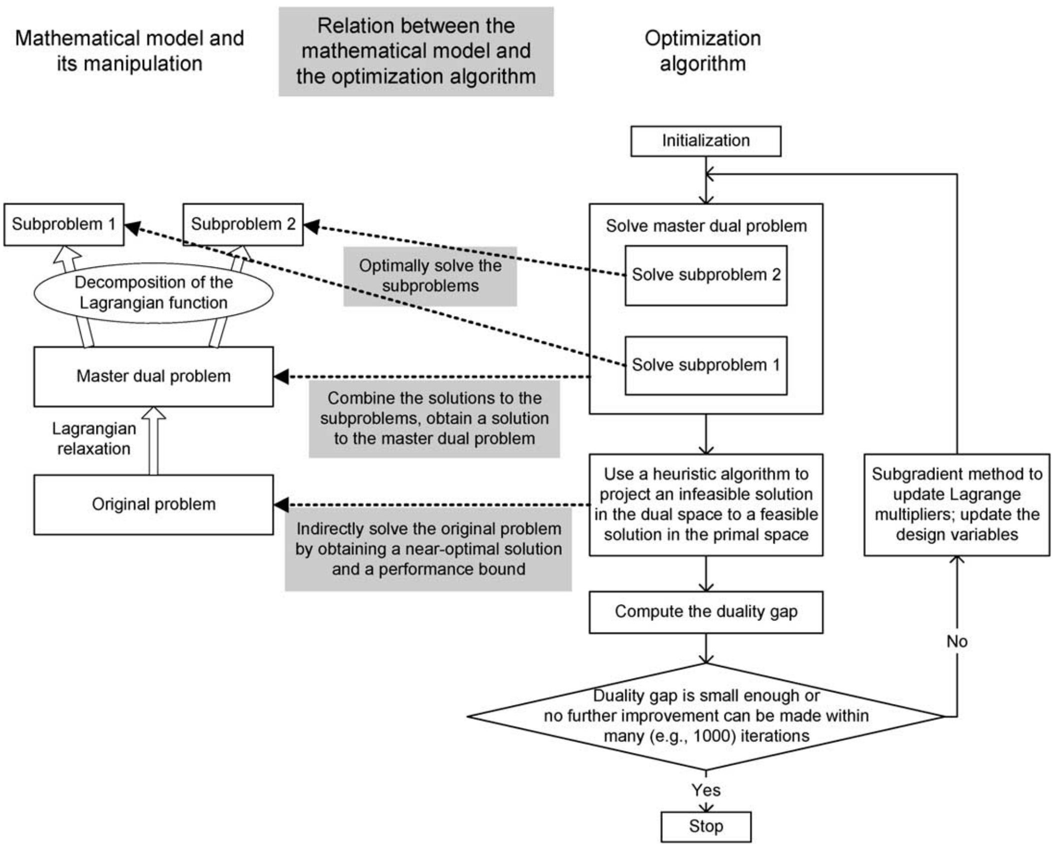


Fig. 1. Illustration of the solution framework.

quantity constraint (10). Corresponding to each constraint, a Lagrange multiplier is introduced and a term is added into the Lagrangian function. The Lagrange multipliers are denoted as $\theta_{sdn}, \pi_j, \xi_{ijc}$ and $\eta_s$ for constraints (4) and (8)–(10), respectively. We propose a novel decomposition that removes the dependence between sub-problems in the Lagrangian function and constraints. The relaxation of the selected constraints leads to the following Lagrangian function $L(\gamma, \upsilon, \alpha, \delta, \phi, \theta, \pi, \xi, \eta)$:

$$\begin{aligned} L(\gamma, \upsilon, \alpha, \delta, \phi, \theta, \pi, \xi, \eta) = {} & \sum_{(p,q)} \sum_{0<z\leqslant Z_{pq}} \gamma_{pqz} P_{pqz} G_{pqz} - \sum_{(p,q)} \sum_{0<z\leqslant Z_{pq}} E_{pqz} - \sum_{(s,d)} \sum_{0<n\leqslant N_{sd}} D_{sdn} \\ & + \sum_{(s,d)} \sum_{0<n\leqslant N_{sd}} \theta_{sdn} \left[ \sum_{(p,q)} \sum_{0<z\leqslant Z_{pq}} \upsilon_{sdn}^{pqz} G_{pqz} - C\alpha_{sdn} \right] \\ & + \sum_j \pi_j \left[ \sum_{(s,d)} \sum_{0<n\leqslant N_{sd}} \phi_j^{sdn} - F_j \right] + \sum_{(i,j)} \sum_{0<c\leqslant n_{ij}} \xi_{ijc} \left[ \sum_{(s,d)} \sum_{0<n\leqslant N_{sd}} \delta_{ijc}^{sdn} - 1 \right] \\ & + \sum_s \eta_s \left[ \sum_d \sum_{0<n\leqslant N_{sd}} \alpha_{sdn} - T_s \right]. \end{aligned} \tag{12}$$

In the Lagrangian function (12), the first three terms are the same as in the primal function, and the last four terms correspond to the four relaxed constraints (4) and (8)–(10), respectively. The maximization of the Lagrangian function is subject to the remaining constraints that are not relaxed, i.e., constraints (5)–(7) and (11).

We define the dual function $q(\theta, \pi, \xi, \eta)$ as the supremum of the Lagrangian function (12). The design variables of the dual problem are the Lagrange multipliers $\theta, \pi, \xi$ and $\eta$. In Appendix A, we prove the following inequality (13), and also prove that the minimum of the dual function is an upper bound of the primal function.

$$\min_{\theta,\pi,\xi,\eta\leqslant 0} q(\theta, \pi, \xi, \eta) \geqslant \max_{\gamma,\upsilon,\alpha,\delta,\phi} L(\gamma, \upsilon, \alpha, \delta, \phi, \theta, \pi, \xi, \eta). \tag{13}$$

After manipulation and re-grouping of the Lagrangian function, we create solvable and separable sub-problems. The details of the manipulation and re-grouping are given in Appendix B. The maximization of the Lagrangian function is transformed to:

$$\sum_{(s,d)} \sum_{0<n\leqslant N_{sd}} \max_{\alpha_{sdn}} \Big\{ \alpha_{sdn} \Big[ H_{sdn} - \min_{\delta,\phi}(Q_{sdn}) \Big] \Big\} + \sum_{(p,q)} \sum_{0<z\leqslant Z_{pq}} \max_{\gamma_{pqz}} \Big\{ \gamma_{pqz} \Big[ P_{pqz} G_{pqz} - \min_{\upsilon}(R_{pqz}) \Big] \Big\} - U, \tag{14}$$

where

$$H_{sdn} = -C\theta_{sdn} + \eta_s - t_s - r_d, \tag{15}$$

$$Q_{sdn} = \sum_{(i,j)} \sum_{0<c\leqslant W} \delta_{ijc}^{sdn}(d_{ijc} - \xi_{ijc}) + \sum_{j} \phi_j^{sdn}(c_j - \pi_j), \tag{16}$$

$$R_{pqz} = \sum_{(s,d)} \sum_{0<n\leqslant N_{sd}} \upsilon_{sdn}^{pqz}(V_{pqz} - \theta_{sdn} G_{pqz}), \tag{17}$$

$$U = \sum_{(i,j)} \sum_{0<c\leqslant W} \xi_{ijc} + \sum_{s} \eta_s T_s. \tag{18}$$

Since the re-grouped Lagrangian function is decomposable, the maximization of the Lagrangian function can be decomposed into sub-problems. There are three groups in (14):

- The first group of (14) represents the design of the lightpath setup status $\alpha$, the lightpath routing and wavelength assignment scheme $\delta$, and the assignment scheme of wavelength converters to lightpaths $\delta$. We call it the *RWA sub-problem*;
- The second group of (14) represents the design of the traffic flow admission status $\gamma$, and the traffic flow routing scheme $\upsilon$. We call it the *traffic flow routing sub-problem*;
- The last group of (14) is independent of any design variables.

### *3.3. Solving the sub-problems*

#### *3.3.1. Solving the RWA sub-problem*

The RWA sub-problem is described as:

$$\max_{\alpha_{sdn}} \Big\{ \alpha_{sdn} \Big[ H_{sdn} - \min_{\delta,\phi}(Q_{sdn}) \Big] \Big\} \quad \text{for all lightpaths } s_{sdn}, \tag{19}$$

subject to the lightpath flow continuity constraints (6), the wavelength conversion constraint (7) and the receiver quantity constraint (11).

Table 1

The algorithm to find the optimal solution for the RWA sub-problem

| | |
|---|---|
| Step 1: | Construct a wavelength graph of the network. The wavelength graph consists of vertices in a matrix-like structure, where each column corresponds to a node of the network, and each row corresponds to a wavelength. In the $c$th ($0 < c \leqslant W$) row, draw a directed edge from the column $i$ to $j$, if $w_{ijc}$ exists, assign weight $(d_{ijc} - \xi_{ijc})$ to the edge to represent the cost of the wavelength channel; otherwise, assign infinite weight to the edge. In the column $i$, draw a directed edge from one row to another row, if a wavelength converter is installed at node $i$, assign weight $(c_i - \pi_i)$ to the edge to represent the cost of the wavelength converter; otherwise, assign infinite weight to the edge |
| Step 2: | Find a shortest path between a given node pair $(s, d)$, and calculate the optimal value of $\min_{\delta,\phi}(Q_{sdn})$ |
| Step 3: | Determine the acceptance or rejection of $s_{sdn}$. If $H_{sdn} > \min_{\delta,\phi}(Q_{sdn})$ and a spare receiver is available at the destination node $d$, then accept $s_{sdn}$ (i.e., set $\alpha_{sdn} = 1$), and assign $s_{sdn}$ with the RWA scheme and the wavelength converter assignment scheme that correspond to the shortest path in the wavelength graph. If $H_{sdn} < \min_{\delta,\phi}(Q_{sdn})$ or there is no spare receiver available at the destination node $d$, then reject $s_{sdn}$ (i.e., set $\alpha_{sdn} = 0$). A tie of $H_{sdn}$ and $\min_{\delta,\phi}(Q_{sdn})$ is broken arbitrarily |

We have developed a method to solve the RWA sub-problem using an existing algorithm for a static RWA problem [22]. By assuming a virtual cost of $w_{ijc}$ as $(d_{ijc} - \xi_{ijc})$, and a virtual cost of a wavelength converter at node $w_{ijc}$ as $(d_{ijc} - \xi_{ijc})$, the meaning of $Q_{sdn}$ can be understood as the total virtual cost of wavelength channels and converters that the lightpath $s_{sdn}$ travels through. So the dual cost of $s_{sdn}$ is $Q_{sdn}$. Note that since $\xi_{ijc} \leqslant 0$, we have $(d_{ijc} - \xi_{ijc}) \geqslant 0$ for all wavelength channels $w_{ijc}$. Similarly, since $\pi_j \leqslant 0$, we have $(c_j - \pi_j) \geqslant 0$ for all intermediate nodes $j$. So, $Q_{sdn} \geqslant 0$. After relaxing the wavelength converter quantity constraint (8), the wavelength channel exclusive usage constraint (9), and the transmitter quantity constraint (10), we are able to sequentially solve the RWA sub-problem for each lightpath, as opposed to considering all lightpaths together. The receiver quantity constraint (11) is ignored first and then we enforce the constraint by using the following policy. For each destination node $d$, the obtained lightpaths are sorted in the ascending order of their minimal dual cost. Lightpath $s_{sdn}$ is only accepted, if its minimal dual cost is less than $H_{sdn}$, and a spare receiver is available at the destination node $d$. Otherwise, this lightpath should be rejected. When multiple lightpaths tie on their minimal dual cost, we break the tie arbitrarily. The algorithm to find the optimal solution for the RWA sub-problem is given in Table 1.

### 3.3.2. *Solving the traffic flow routing sub-problem*

The traffic flow routing sub-problem is:

$$\max_{\gamma_{pqz}}\left\{\gamma_{pqz}\left[P_{pqz}G_{pqz} - \min_{\upsilon}(R_{pqz})\right]\right\} \quad \text{for all traffic flows } \chi_{pqz}, \tag{20}$$

subject to the traffic flow continuity constraint (5).

This sub-problem requires the selection of traffic flows based on their profitability. We evaluate the profitability of a traffic flow based on the resources that the traffic flow requires in both the electrical and optical domains. By assuming a virtual cost of lightpath $s_{sdn}$ as $(V_{pqz} - \theta_{sdn}G_{pqz})$, the meaning of $R_{pqz}$ can be understood as the total virtual cost of lightpaths that the traffic flow $\chi_{pqz}$ travels through. So the dual cost of $\chi_{pqz}$ is $R_{pqz}$. Note that since $\theta_{sdn} \leqslant 0$, we have $(V_{pqz} - \theta_{sdn}G_{pqz}) \geqslant 0$ for all lightpaths $s_{sdn}$. So, $R_{pqz} \geqslant 0$. We can obtain the minimal dual cost by sequentially using Dijkstra's shortest path algorithm for each traffic flow. The minimal dual cost of $\chi_{pqz}$ is compared to the revenue $P_{pqz}G_{pqz}$ that $\chi_{pqz}$ generates if it is accepted. A routing scheme $\upsilon$ is obtained for each accepted traffic flow.

## 3.4. *Solving the dual problem*

We use a subgradient-based method to coordinate the solutions of the sub-problems. The sub-problems are linked together by the Lagrange multipliers, which are updated in iterations. We create a compound vector of the Lagrange multipliers $(\theta, \pi, \xi, \eta)$, where $\theta, \pi, \xi$ and $\eta$ denote the vectors of the Lagrange multipliers $(\theta_{sdn})$ for all lightpaths $s_{sdn}$, $(\pi_j)$ for all intermediate nodes $j$, $(\xi_{ijc})$ for all wavelength channels $w_{ijc}$and $(\eta_s)$ for all source nodes $s$. We update $(\theta, \pi, \xi, \eta)$ in iterations towards the direction of its subgradient.

$$(\theta, \pi, \xi, \eta)^{(h+1)} = (\theta, \pi, \xi, \eta)^{(h)} + \beta^{(h)} g\big((\theta, \pi, \xi, \eta)^{(h)}\big), \tag{21}$$

where $(\theta, \pi, \xi, \eta)^{(h)}$ denotes the value of vectors $(\theta, \pi, \xi, \eta)$ obtained in the $h$th iteration, and $\beta^{(h)}$ denotes the step size for the $(h+1)$th iteration.

The subgradient of $q$ in Eq. (13) is denoted as $(g(\theta), g(\pi), g(\xi), g(\eta))$. The vectors $g(\theta), g(\pi), g(\xi)$ and $g(\eta)$ comprise $(g(\theta_{sdn}))$ for all lightpaths $s_{sdn}$, $(g(\pi_j))$ for all intermediate nodes $j$, $(g(\xi_{ijc}))$ for all wavelength channels $w_{ijc}$ and $(g(\eta_s))$ for all source nodes $s$, respectively. We have the subgradient components:

$$g(\theta_{sdn}) = \sum_{(p,q)} \sum_{0<z\leqslant Z_{pq}} v_{sdn}^{pqz} G_{pqz} - C\alpha_{sdn} \quad \text{for all lightpaths } s_{sdn}, \tag{22}$$

$$g(\pi_j) = \sum_{(s,d)} \sum_{0<n\leqslant N_{sd}} \phi_j^{sdn} - F_j \quad \text{for all intermediate nodes } j, \tag{23}$$

$$g(\xi_{ijc}) = \sum_{(s,d)} \sum_{0<n\leqslant N_{sd}} \delta_{ijc}^{sdn} - 1 \quad \text{for all wavelength channels } w_{ijc}, \tag{24}$$

$$g(\eta_s) = \sum_{d} \sum_{0<n\leqslant N_{sd}} \alpha_{sdn} - T_s \quad \text{for all source nodes } s. \tag{25}$$

The subgradient terms in Eqs (22)–(25) correspond to the relaxed constraints (4) and (8)–(10).

The step size for the iterative updates is computed as

$$\beta^{(h)} = \mu \times \frac{q^U - q^{(h)}}{g^T((\theta, \pi, \xi, \eta)^{(h)}) g((\theta, \pi, \xi, \eta)^{(h)})}, \tag{26}$$

where $q^U$ is an approximation to the optimal dual value. We set an initial estimation of $q^U$ to the value of the objective function $f$ for a feasible solution. $q^{(h)}$ is the value of the dual function $q$ at the $h$th iteration. The range of the parameter $\mu$ is $0 < \mu < 2$, which is adjusted adaptively as the algorithm converges. Specifically, if the value of $q^{(h)}$ remains unchanged in 3 consecutive iterations, the value of $\mu$ is decreased by a factor $p < 1$, and if the value of $q^{(h)}$ increases in 5 consecutive iterations, the value of $\mu$ is increased by a factor $1/p$. From our simulation, fast convergence is achieved when $p = 0.95$. The vector $g^{\mathrm{T}}((\theta, \pi, \xi, \eta)^{(h)})$ is the transpose of the vector $g((\theta, \pi, \xi, \eta)^{(h)})$. The value $q^U$ is also updated when a lower $f$ value is obtained.

### 3.5. Constructing a feasible solution

A heuristic algorithm is developed to construct a feasible solution for the primal problem. Because some constraints for the primal problem are relaxed and transformed into the price terms in the dual problem, the solution to the dual problem is generally infeasible, i.e., some constraints are violated. Our heuristic algorithm repeatedly diverts the least profitable traffic flows and the traffic flows along the least profitable lightpaths onto other existing lightpaths, until all conflicts are resolved. The description of the heuristic algorithm is given in Table 2.

### 3.6. Computational complexity analysis

The computational complexities to solve the traffic flow routing and RWA sub-problems are $O(A(N+W)N^2W)$ and $O(ZA^2N^2)$, respectively, where $A$ is the total number of potential lightpaths to be set up; $N$ is the number

Table 2

A heuristic algorithm to construct a feasible solution for the primal problem

1.0 (Rough searching stage. Transform an infeasible RWA scheme obtained in the dual solution to a feasible but not very optimized RWA scheme. At the same time, obtain a rough traffic routing scheme, which is feasible but far from being optimized.)

1.1 (Initial RWA. Deploy lightpaths one-by-one.)

1.1.1 (Choose the top priority lightpath from the lightpaths that have not been deployed or rejected. If two lightpaths tie on the first priority, use the second priority and then the third priority to break the tie; if still tie, break the tie randomly.)

Priority 1: Descending order of the profit of a lightpath in the dual problem, which is calculated by subtracting the dual cost $Q_{sdn}$ of the lightpath $s_{sdn}$ from the total revenue of the unsatisfied traffic flows between $(s, d)$. The total revenue of the unsatisfied traffic flows between $(s, d)$ is estimated as the total revenue of the traffic flows between $(s, d)$ minus $m \times 0.8 \times C$, where $m$ is the number of existing lightpaths between $(s, d)$, and $C$ is the capacity of a lightpath. Here, we assume existing lightpaths use 80% capacity to carry traffic flows;
Priority 2: Ascending order of the number of the constraints that are violated by a lightpath;
Priority 3: If a lightpath is set up in the dual solution, then it has higher priority than the lightpath that is not set up in the dual solution.

1.1.2 (Deploy the top priority lightpath. Use the first policy to deploy the lightpath, if the required resources are available so far. If failed, use the second policy and then the third policy. If still failed, reject the lightpath.)

Policy 1: Deploy the lightpath based on its RWA scheme obtained in the dual solution;
Policy 2: Deploy the lightpath based on its routing scheme obtained in the dual solution, but choose a different wavelength assignment scheme;
Policy 3: Compute a new relatively low cost RWA scheme for the lightpath.

1.1.3 If there are lightpaths that have not been deployed or rejected, then repeat from Step 1.1.1.

1.2 (Traffic routing.)

1.2.1 (Sort traffic flows. If two traffic flows tie on the first priority, use the second priority and then the third priority to break the tie; if still tie, break the tie arbitrarily.)

Priority 1: Descending order of the profit of a traffic flow per bandwidth unit, which is calculated by subtracting the dual cost $R_{pqz}$ of $\chi_{pqz}$ from its revenue $P_{pqz}G_{pqz}$, then dividing by its bandwidth requirement $G_{pqz}$;
Priority 2: Ascending order of the number of the constraints that are violated by a traffic flow;
Priority 3: Descending order of the bandwidth requirement $G_{pqz}$ of $\chi_{pqz}$.

1.2.2 (Deploy traffic flows one-by-one based on the sorted order. Use the first policy to deploy a traffic flow, if the required resources are available so far. If failed, use the second policy. If still failed, then reject the traffic flow.)

Policy 1: Deploy a traffic flow based on its traffic routing scheme obtained in the dual solution.
Policy 2: Compute a new relatively low cost traffic routing scheme for traffic flow.

1.3 (RWA adjustment.)

1.3.1 Remove non-profitable lightpaths.
1.3.2 Re-route the traffic flows that use the disconnected lightpaths. If not re-routed, then reject the traffic flows.

2.0 (Extensive searching stage. Optimize the traffic routing scheme based on the virtual topology obtained in the previous rough searching stage.)

Use the Lagrangian relaxation and subgradient methods to solve the optimization problem:

$$\max_{\gamma,\upsilon}(f), \quad \text{where } f = \sum_{(p,q)} \sum_{0<z\leqslant Z_{pq}} \gamma_{pqz} P_{pqz} G_{pqz} - \sum_{(p,q)} \sum_{0<z\leqslant Z_{pq}} E_{pqz}. \tag{27}$$

Subject to the lightpath capacity constraint (4), and the traffic flow continuity constraint (5). The solution method of this optimization problem is available in [23].

of nodes; and $Z$ is the number of traffic flows. Thus the computation complexity to solve the dual problem is $O(A(N+W)N^2W)+O(ZA^2N^2)$. The dual problem needs to be solved for many iterations in the overall framework. The good convergence of the subgradient-based iterations keeps the computational complexity of the overall optimization approach at an acceptable level. Our simulation on practical scale networks demonstrates the efficiency of the approach.

## 4. Numeric results

### *4.1. Verification of the proposed solution method*

The complexity of the problem is very high. Table 3 shows the number of variables and constraints for three sample networks. Even for the first small sample network, the computation complexity is so high that CPLEX cannot obtain the optimal solution within a reasonable time. Our method is verified by a comparison to the best known results in the literature for the first sample network. Our method can obtain near-optimal solution (and a performance bound) within a short computation time. Then, two practical scale networks are used to examine the impact of cost parameters to the profit objective.

When eliminating the cost aspects and setting all the revenue coefficients $P_{pqz}$ to one in our objective function (1), we simplify the objective function as:

$$\max_{\gamma,\upsilon,\alpha,\delta,\phi}(f), \quad \text{where } f=\sum_{(p,q)}\sum_{0<z\leqslant Z_{pq}}\gamma_{pqz}G_{pqz}. \tag{28}$$

Our algorithm is verified by using this simplified objective, because optimization results are available for this objective using other approaches [8]. It was attempted to use CPLEX to obtain the optimal solution for the first sample network [8], whose topology is shown in Fig. 2, and traffic pattern is shown in Tables 4–6. The horizontal and vertical indexes are the source and destination nodes, respectively. Although theoretically CPLEX's branch-and-bound solution technique can obtain the optimal solution, in practice, CPLEX is unable to handle this problem, because of the complexity of the problem and the inefficiency of CPLEX's method. Even for this small network, CPLEX computation is so time consuming that it had to be terminated after running for a long time, and in many

Table 3
Number of variables and constraints of the profit optimization problem for three sample networks

| Network and traffic properties | | | | Number of integer variables | Number of constraints |
|---|---|---|---|---|---|
| Nodes | Links | Wavelengths | Traffic flows | | |
| 6 | 8 | 4 | 390 | 13,926 | 626 |
| 14 | 21 | 32 | 1321 | 1,341,289 | 6053 |
| 22 | 35 | 32 | 2202 | 3,723,962 | 10,086 |

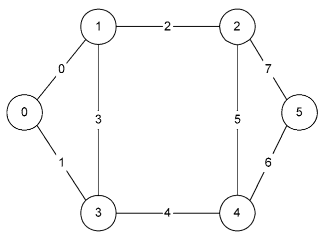


Fig. 2. The first sample network with 6 nodes and 8 links.

Table 4
Traffic flows of 1 bandwidth unit for the first sample network

| | | | | | |
|---|---|---|---|---|---|
| 0 | 5 | 4 | 11 | 12 | 9 |
| 0 | 0 | 8 | 5 | 16 | 6 |
| 14 | 12 | 0 | 9 | 6 | 16 |
| 4 | 11 | 15 | 0 | 1 | 5 |
| 10 | 2 | 3 | 3 | 0 | 9 |
| 2 | 1 | 8 | 15 | 13 | 0 |

Table 5
Traffic flows of 3 bandwidth units for the first sample network

| | | | | | |
|---|---|---|---|---|---|
| 0 | 6 | 2 | 1 | 5 | 4 |
| 8 | 0 | 8 | 6 | 7 | 8 |
| 1 | 3 | 0 | 0 | 2 | 7 |
| 5 | 7 | 3 | 0 | 2 | 6 |
| 6 | 4 | 5 | 0 | 0 | 2 |
| 5 | 4 | 4 | 2 | 0 | 0 |

Table 6
Traffic flows of 12 bandwidth units for the first sample network

| | | | | | |
|---|---|---|---|---|---|
| 0 | 1 | 1 | 1 | 0 | 0 |
| 1 | 0 | 1 | 1 | 0 | 2 |
| 0 | 1 | 0 | 2 | 1 | 0 |
| 2 | 0 | 2 | 0 | 2 | 0 |
| 1 | 2 | 0 | 2 | 0 | 1 |
| 1 | 1 | 2 | 2 | 2 | 0 |

Table 7
A comparison between our results and the published results

| | Near-optimal results by terminating CPLEX computations after a long running time | Maximizing single-hop traffic heuristics results | Maximizing resource utilization heuristics results | **The results obtained by our proposed method** | The upper bound obtained by our method |
|---|---|---|---|---|---|
| $T = 2, W = 3$ | – | – | – | **516** | 576 |
| $T = 3, W = 3$ | 738 | 701 | 666 | **751** | 851 |
| $T = 4, W = 4$ | 927 | 883 | 925 | **930** | 976 |
| $T = 5, W = 3$ | 967 | 933 | 933 | **969** | 987 |
| $T = 7, W = 3$ | 967 | 933 | 933 | **969** | 987 |
| $T = 3, W = 4$ | 738 | 701 | 666 | **751** | 851 |
| $T = 4, W = 4$ | 933 | 920 | 925 | **930** | 976 |
| $T = 5, W = 4$ | 988 | 988 | 988 | **988** | 988 |

*Note*: Larger optimization results mean better throughput. The first three columns are the best known results in the literature.

cases no optimal solution was obtained in [8]. Our method uses a reasonable computational time (about 10 minutes for this sample network) to obtain comparable results (shown in Table 7). It is assumed that all nodes have the same number of transmitters and receivers, i.e., $T_i = R_i = T$ for all node $i$. In addition, we obtain an upper bound of the objective function at the same time.

## *4.2. Optimization results for practical scale networks*

We study the impact of cost parameters to the profit for NSFNET, whose topology is shown in Fig. 3. The randomly generated traffic pattern is shown in Tables 8–10. We found that the uniformly distributed traffic pattern is more challenging than other special patterns. Therefore, we evaluate our algorithm for the uniform traffic pattern. We fix other cost parameters and investigate the impact of a single cost parameter. Between each node pair, there are traffic flows with three different bandwidths. Our algorithm accepts or rejects traffic flows between the same node pair independently based on the profit objective. The accepted traffic flows are allowed to use different traffic routing schemes.

We study the impact of the number of transmitters and receivers on the profit. It is assumed that all nodes have the same number of transmitters and receivers, i.e., $T_i = R_i = T$ for all node $i$. For now, we do not consider the traffic grooming cost $V$. All revenue coefficients $P_{pqz}$ are set to one, which means the revenue is proportional to the bandwidth requirement. Since the total traffic volume counts to 6148 bandwidth units, the maximal revenue is 6148, if all the traffic flows are accepted. Figure 4 illustrates the achieved profit and its upper bound with respect to the number of transmitters at a node. We can see that as the number of transmitters increases, the profit increases. The increasing rate of profit is approximately linear to the number of transmitters before the transmitters become abundant. After that, adding more transmitters increases the cost but contributes no additional revenue. The profit decreases at a rate approximately linear to the transmitter cost. In this way, the optimal number of transmitters at a node is obtained for a given traffic pattern. Figure 5 shows the percentage of the rejected traffic flows as the transmitter cost increases. The number of transmitters and receivers at a node is set to the

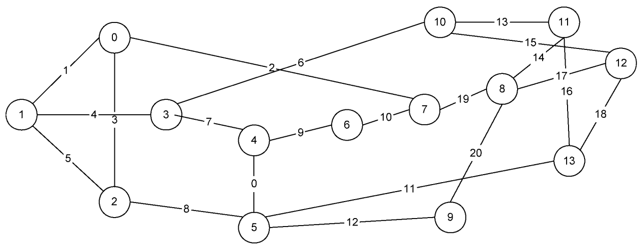

Fig. 3. 14-node NSFNET topology.

Table 8
Traffic flows of 1 bandwidth unit for NSFNET (total 541 flows)

| | | | | | | | | | | | | | |
|---|---|---|---|---|---|---|---|---|---|---|---|---|---|
| 0 | 6 | 3 | 12 | 5 | 1 | 6 | 0 | 2 | 0 | 4 | 2 | 0 | 3 |
| 0 | 0 | 2 | 2 | 2 | 11 | 1 | 1 | 1 | 2 | 3 | 0 | 1 | 3 |
| 3 | 2 | 0 | 3 | 0 | 1 | 2 | 3 | 11 | 3 | 1 | 2 | 2 | 0 |
| 3 | 1 | 4 | 0 | 11 | 1 | 2 | 3 | 2 | 2 | 1 | 2 | 1 | 3 |
| 1 | 3 | 0 | 2 | 0 | 4 | 0 | 2 | 0 | 3 | 0 | 1 | 1 | 3 |
| 1 | 2 | 1 | 3 | 2 | 0 | 1 | 3 | 3 | 11 | 0 | 6 | 10 | 9 |
| 2 | 2 | 3 | 1 | 10 | 3 | 0 | 0 | 3 | 1 | 2 | 0 | 3 | 7 |
| 3 | 10 | 2 | 3 | 5 | 4 | 1 | 0 | 0 | 3 | 2 | 0 | 3 | 0 |
| 3 | 0 | 12 | 3 | 3 | 3 | 1 | 0 | 0 | 2 | 1 | 7 | 9 | 0 |
| 0 | 0 | 0 | 1 | 2 | 0 | 2 | 0 | 1 | 0 | 1 | 0 | 0 | 4 |
| 4 | 0 | 0 | 10 | 0 | 3 | 0 | 6 | 0 | 3 | 0 | 3 | 5 | 3 |
| 2 | 3 | 1 | 1 | 3 | 2 | 13 | 2 | 10 | 2 | 2 | 0 | 1 | 3 |
| 13 | 0 | 11 | 2 | 0 | 1 | 2 | 0 | 9 | 0 | 2 | 1 | 0 | 3 |
| 10 | 14 | 0 | 15 | 9 | 3 | 1 | 3 | 0 | 12 | 2 | 1 | 3 | 0 |

Table 9

Traffic flows of 3 bandwidth units for NSFNET (total 417 flows)

| | | | | | | | | | | | | | |
|---|---|---|---|---|---|---|---|---|---|---|---|---|---|
| 0 | 1 | 2 | 1 | 3 | 1 | 0 | 2 | 2 | 0 | 3 | 2 | 0 | 4 |
| 3 | 0 | 0 | 2 | 2 | 2 | 1 | 1 | 1 | 2 | 3 | 0 | 1 | 6 |
| 1 | 2 | 0 | 1 | 0 | 2 | 2 | 3 | 1 | 2 | 3 | 8 | 6 | 7 |
| 6 | 1 | 0 | 0 | 1 | 3 | 2 | 1 | 2 | 2 | 1 | 2 | 1 | 8 |
| 1 | 2 | 7 | 2 | 0 | 1 | 0 | 2 | 0 | 6 | 0 | 8 | 2 | 5 |
| 5 | 4 | 1 | 1 | 2 | 0 | 1 | 1 | 3 | 4 | 0 | 1 | 1 | 2 |
| 2 | 5 | 7 | 8 | 1 | 2 | 0 | 0 | 3 | 1 | 2 | 0 | 0 | 5 |
| 2 | 3 | 2 | 1 | 3 | 4 | 5 | 0 | 0 | 1 | 2 | 0 | 7 | 6 |
| 1 | 0 | 5 | 5 | 2 | 1 | 2 | 0 | 0 | 2 | 1 | 3 | 1 | 2 |
| 0 | 0 | 6 | 1 | 2 | 0 | 2 | 0 | 3 | 0 | 2 | 0 | 0 | 1 |
| 1 | 4 | 7 | 3 | 0 | 0 | 3 | 3 | 0 | 1 | 0 | 1 | 1 | 2 |
| 2 | 3 | 2 | 5 | 6 | 7 | 8 | 2 | 2 | 2 | 2 | 0 | 1 | 1 |
| 0 | 0 | 1 | 2 | 2 | 3 | 4 | 0 | 1 | 0 | 3 | 5 | 0 | 7 |
| 4 | 3 | 0 | 2 | 3 | 3 | 3 | 1 | 0 | 4 | 7 | 1 | 0 | 0 |

Table 10

Traffic flows of 12 bandwidth units for NSFNET (total 363 flows)

| | | | | | | | | | | | | | |
|---|---|---|---|---|---|---|---|---|---|---|---|---|---|
| 0 | 2 | 5 | 3 | 5 | 4 | 2 | 1 | 2 | 5 | 2 | 1 | 5 | 0 |
| 4 | 0 | 4 | 1 | 4 | 3 | 2 | 5 | 3 | 4 | 3 | 3 | 1 | 3 |
| 0 | 1 | 0 | 0 | 0 | 2 | 3 | 0 | 5 | 3 | 2 | 1 | 0 | 2 |
| 1 | 1 | 0 | 0 | 3 | 1 | 1 | 0 | 2 | 4 | 4 | 3 | 1 | 4 |
| 3 | 0 | 0 | 2 | 0 | 3 | 5 | 2 | 4 | 2 | 5 | 4 | 0 | 3 |
| 1 | 3 | 2 | 0 | 1 | 0 | 2 | 0 | 0 | 1 | 0 | 1 | 5 | 2 |
| 1 | 4 | 0 | 4 | 0 | 0 | 0 | 0 | 4 | 3 | 1 | 2 | 2 | 1 |
| 0 | 3 | 1 | 0 | 5 | 0 | 4 | 0 | 0 | 0 | 3 | 0 | 4 | 0 |
| 0 | 4 | 1 | 2 | 3 | 5 | 1 | 4 | 0 | 2 | 1 | 5 | 4 | 0 |
| 5 | 1 | 0 | 1 | 1 | 4 | 0 | 0 | 1 | 0 | 1 | 0 | 0 | 1 |
| 1 | 3 | 3 | 0 | 4 | 3 | 1 | 2 | 0 | 0 | 0 | 0 | 1 | 3 |
| 1 | 0 | 2 | 2 | 5 | 1 | 0 | 3 | 3 | 3 | 2 | 0 | 3 | 5 |
| 0 | 5 | 2 | 3 | 4 | 1 | 2 | 0 | 2 | 1 | 1 | 1 | 0 | 3 |
| 5 | 2 | 5 | 5 | 1 | 0 | 2 | 0 | 1 | 4 | 0 | 1 | 0 | 0 |

optimal value 9 that is obtained in Fig. 4. It is assumed that the transmitter cost and the receiver cost are the same.

We next study the impact of the wavelength channel cost. With an increase of the wavelength channel cost, the total number of the established lightpaths decreases (shown in Fig. 6). When the wavelength channel cost increases from 0 to 9, the total number of established lightpaths decreases by $(119-88)/119 = 26\%$. The reason is that more lightpaths become non-profitable as the wavelength channel cost increases. The remaining profitable traffic flows tend to be packed into a smaller number of lightpaths. An increase of the wavelength channel cost dramatically reduces the lightpaths that use multiple fibre hops. In Fig. 7, we show that the percentage of 3-fibre hop lightpaths is reduced from 45 to 23%, as the wavelength channel cost increases from 0 to 9. This is because more lightpaths of single fibre hop are established when the wavelength channel cost is high. The proportion of single-hop lightpaths increases from 18 to 41%, as the wavelength channel cost increases from 0 to 9.

We study the impact of the traffic grooming cost. The optical layer cost is fixed. The traffic grooming cost is modelled by the coefficient $V_{pqz}$. We set $V_{pqz}$ to a fraction of the bandwidth requirement $G_{pqz}$ of $\chi_{pqz}$. Table 11 shows the number of the accepted traffic flows with different bandwidths. When the traffic grooming

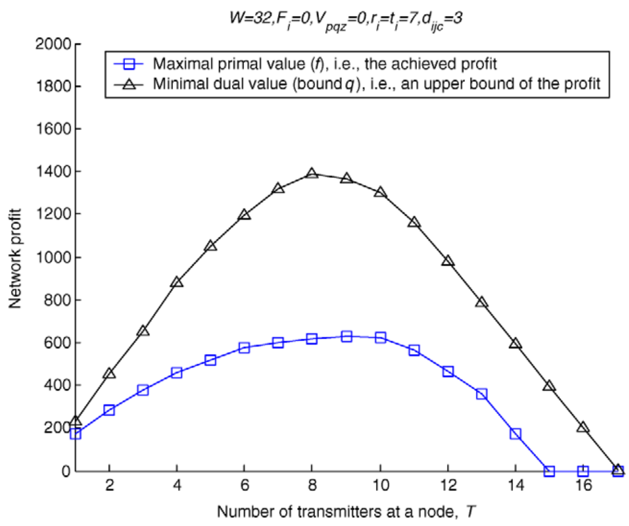


Fig. 4. Profit and an upper bound w.r.t. the number of transmitters at a node.

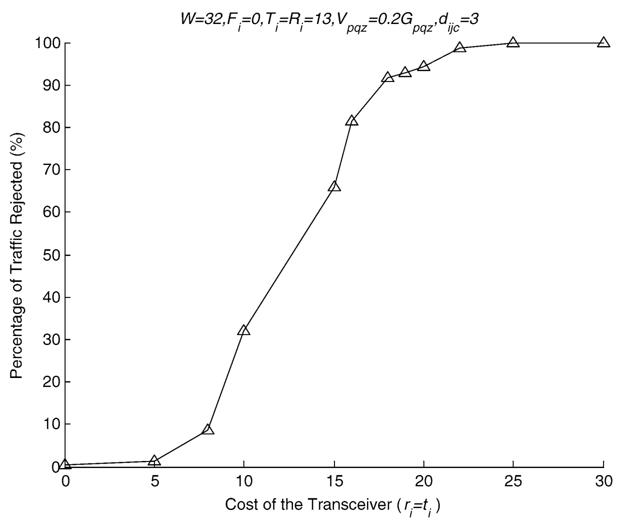


Fig. 5. Percentage of the rejected traffic flows w.r.t. the transmitter cost.

cost $V_{pqz}$ increases from 0 to $0.6G_{pqz}$, the traffic flows with different bandwidths exhibit dramatically different behaviours: (1) for large bandwidth (i.e., OC-12) traffic flows, the number of traffic flows using multiple hop lightpath decreases significantly, by $(29 - 7)/29 = 76\%$; the number of traffic flows using single hop lightpath slightly decreases, by $(261 - 250)/261 = 4\%$. It is more efficient to carry them by single hop lightpaths; (2) for medium bandwidth (i.e., OC-3) traffic flows, the number of traffic flows using multiple hop lightpaths decreases by $(81 - 59)/81 = 27\%$; the number of traffic flows using single hop lightpath increases slightly, by $(274 - 246)/246 = 11\%$. More lightpaths should be set up so that more such traffic flows can be carried over single hop lightpaths. However, the revenue generated by such traffic flows remains at the same level; (3) for small bandwidth (i.e., OC-1) traffic flows, the number of traffic flows using multiple hop lightpaths increases significantly, by $(139 - 45)/45 = 209\%$; the number of traffic flows using single hop lightpaths approximately remains the same. More such traffic flows are accepted by using multiple hop lightpaths (particularly two hop lightpaths).

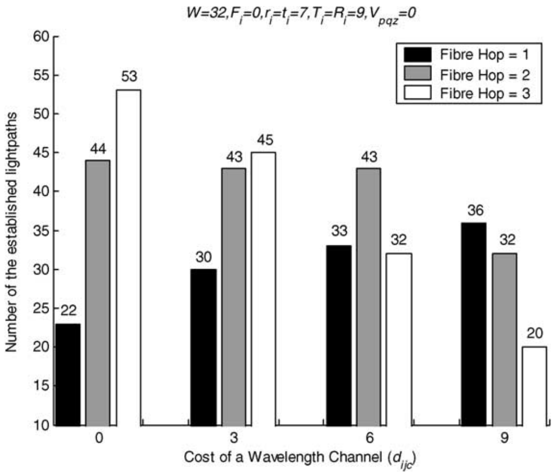


Fig. 6. Number of the established lightpaths of different fibre hops w.r.t. the wavelength channel cost.

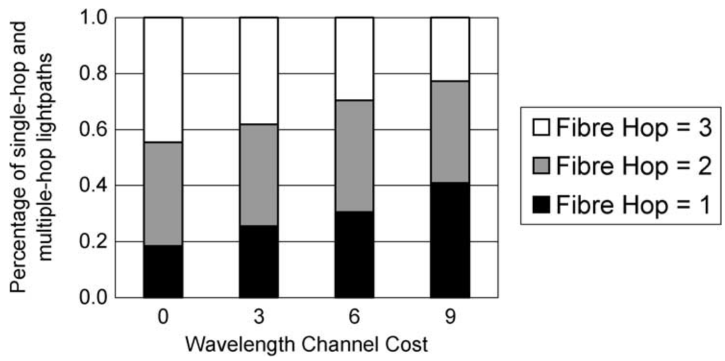


Fig. 7. Percentage of single-hop and multiple-hop lightpaths in all established lightpaths w.r.t. the wavelength channel cost.

Table 11

Total number of the accepted traffic flows of different bandwidth

| Traffic flow bandwidth | Lightpath hop | $V_{pqz} = 0$ | $V_{pqz} = 0.6 \times G_{pqz}$ |
|---|---|---|---|
| OC-12 (Total 363 traffic flows) | 1 | 261 | 250 |
| | 2 | 29 | 7 |
| | 3 | 0 | 0 |
| | 4 | 0 | 0 |
| OC-3 (Total 417 traffic flows) | 1 | 246 | 274 |
| | 2 | 81 | 59 |
| | 3 | 3 | 1 |
| | 4 | 0 | 0 |
| OC-1 (Total 541 traffic flows) | 1 | 350 | 352 |
| | 2 | 45 | 139 |
| | 3 | 9 | 9 |
| | 4 | 1 | 0 |

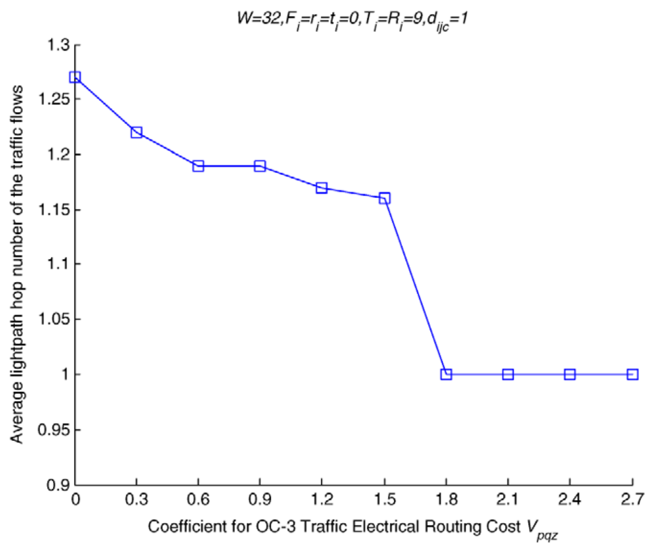


Fig. 8. Average lightpath hops of OC-3 traffic flows w.r.t. their traffic grooming cost.

The reason is that such traffic flows use the segregated bandwidth that cannot be used by medium and large bandwidth traffic flows. Since we assume that the traffic grooming cost is proportional to the bandwidth requirement, the traffic grooming cost for small bandwidth traffic flows is not a major cost compared to other costs such as the optical layer cost.

We study the ratio of optical pass-through traffic at a node with respect to the traffic grooming cost. We fix the traffic grooming cost $V_{pqz}$ for OC-1 and OC-12 traffic flows to 0.1 and 1.2, respectively, and vary $V_{pqz}$ for OC-3 traffic flows. We observe that as $V_{pqz}$ increases, the average number of lightpath hops of OC-3 traffic flows decreases (shown in Fig. 8). When $V_{pqz}$ reaches 1.5, all OC-3 traffic flows are carried over single hop lightpaths. The reason is that the revenue of an OC-3 traffic flow is 3 when $P_{pqz} = 1$. When $V_{pqz}$ reaches 1.5, the traffic flows cannot afford to take two lightpath hops anymore. Since the vast majority of OC-3 traffic flows are carried by single hop or two-hop lightpaths as shown in Table 11, we have the rough relation of the average lightpath hop number and the percentage of optical pass-through traffic flows:

$$\begin{aligned}&\text{Average lightpath hop number of a traffic flow}\\&\quad = 1 + (\text{Optical passthrough traffic flows at a node})\%. \end{aligned} \tag{29}$$

The results in Fig. 8 indicate that about 15–20% OC-3 traffic flows optically pass through intermediate nodes, when the $V_{pqz}$ is below 1.5. The remaining 80–85% OC-3 traffic flows exit from add-drop ports of an optical switch. They either reach their final destination, or are re-groomed with other traffic flows and re-enter the optical domain again.

Our results show that when wavelength converters are used, their contribution to the profit objective is negligible. In Table 12, the influence of the number of wavelength converters at a node on the profit objective is shown. Compared to the counter cases of no wavelength converters, the profit improvement is marginal.

For most cases in the second sample network, our method can compute results within 2 hours on a PC configured with a 1.4 GHz Intel® CPU, 512 MB RAM and the Windows XP® operating system.

We study the network profit optimization problem for the third sample network. This network has 22 nodes, 35 links and 32 wavelengths on each link. The topology is shown in Fig. 9. The uniform traffic pattern is shown in Tables 13–15, counting to 2202 traffic flows in total. The trafficg grooming problem in WDM

Table 12

Influence of the number of wavelength converters at a node on the profit objective

| $W$ | $T_i, R_i$ | $d_{ijc}$ | $r_i, t_i$ | $V_{pqz}$ | | | $F_i$ | $c_i$ | $f$ |
|---|---|---|---|---|---|---|---|---|---|
| | | | | OC-1 | OC-3 | OC-12 | | | |
| 32 | 9 | 0 | 7 | 0 | 0 | 0 | 0 | 0 | **1402** |
| 32 | 9 | 0 | 7 | 0 | 0 | 0 | 1 | 0.01 | **1413** |
| 32 | 9 | 0.2 | 7 | 0 | 0 | 0 | 0 | 0 | **1386** |
| 32 | 9 | 0.2 | 7 | 0 | 0 | 0 | 1 | 0.01 | **1388** |
| 32 | 9 | 3 | 7 | 0 | 0 | 0 | 0 | 0 | **690** |
| 32 | 9 | 3 | 7 | 0 | 0 | 0 | 1 | 0.01 | **699** |
| 32 | 9 | 3 | 7 | 0.1 | 0.3 | 1.2 | 0 | 0 | **127** |
| 32 | 9 | 3 | 7 | 0.1 | 0.3 | 1.2 | 1 | 0.01 | **127** |

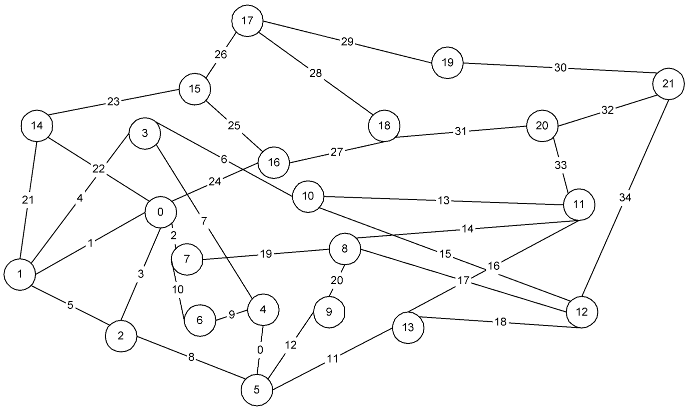

Fig. 9. The third sample network with 22 nodes and 35 links.

networks has never been studied for such large networks before, because the limitation of the existing optimization algorithm. Our method can compute a feasible solution and a performance bound within 5–6 hours. In Fig. 10, we show that the network profit decreases as the cost of a transmitter and receiver increases.

## 5. Conclusions

In this study of static traffic grooming in WDM networks, we have modeled the profit as the surplus of the revenue generated by the accepted traffic flows over resource costs. With a profit optimization objective that incorporates both cost minimization and throughput maximization objectives, we can identify profitable traffic flows, and provide optimized provisioning schemes for the accepted traffic flows. Using the LR and subgradient methods, we can solve the optimization problem for fairly large networks. Our approach can obtain an upper bound to evaluate the optimality of the feasible solution. A comparison between our results and the published results demonstrates the effectiveness of our approach. In studying a practical-size network, we have observed different behaviours and contributions to the profit objective by different bandwidth traffic flows, and when the relative cost of electrical and optical layers changes. In addition, our study has shown that the use of wavelength converters has little contribution to the profit objective for static traffic patterns.

Table 13

Traffic flows of 1 bandwidth unit for the third sample network

| | | | | | | | | | | | | | | | | | | | | | |
|---|---|---|---|---|---|---|---|---|---|---|---|---|---|---|---|---|---|---|---|---|---|
| 0 | 6 | 3 | 12 | 5 | 1 | 6 | 0 | 2 | 0 | 4 | 2 | 0 | 3 | 6 | 0 | 2 | 0 | 4 | 2 | 0 | 3 |
| 0 | 0 | 2 | 2 | 2 | 11 | 1 | 1 | 1 | 2 | 3 | 0 | 1 | 3 | 3 | 0 | 2 | 0 | 4 | 0 | 2 | 6 |
| 3 | 2 | 0 | 3 | 0 | 1 | 2 | 3 | 11 | 3 | 1 | 2 | 2 | 0 | 1 | 3 | 0 | 2 | 0 | 4 | 0 | 2 |
| 3 | 1 | 4 | 0 | 11 | 1 | 2 | 3 | 2 | 2 | 1 | 2 | 1 | 3 | 3 | 1 | 10 | 3 | 0 | 0 | 3 | 1 |
| 1 | 3 | 0 | 2 | 0 | 4 | 0 | 2 | 0 | 3 | 0 | 1 | 1 | 3 | 0 | 9 | 3 | 1 | 3 | 0 | 12 | 7 |
| 1 | 2 | 1 | 3 | 2 | 0 | 1 | 3 | 3 | 11 | 0 | 6 | 10 | 9 | 3 | 1 | 4 | 0 | 11 | 1 | 2 | 3 |
| 2 | 2 | 3 | 1 | 10 | 3 | 0 | 0 | 3 | 1 | 2 | 0 | 3 | 7 | 2 | 3 | 5 | 4 | 1 | 0 | 0 | 4 |
| 3 | 10 | 2 | 3 | 5 | 4 | 1 | 0 | 0 | 3 | 2 | 0 | 3 | 0 | 3 | 1 | 1 | 3 | 2 | 0 | 2 | 10 |
| 3 | 0 | 12 | 3 | 3 | 3 | 1 | 0 | 0 | 2 | 1 | 7 | 9 | 0 | 11 | 2 | 0 | 1 | 2 | 0 | 9 | 0 |
| 0 | 0 | 0 | 1 | 2 | 0 | 2 | 0 | 1 | 0 | 1 | 0 | 0 | 4 | 6 | 0 | 3 | 0 | 3 | 5 | 3 | 0 |
| 4 | 0 | 0 | 10 | 0 | 3 | 0 | 6 | 0 | 3 | 0 | 3 | 5 | 3 | 0 | 2 | 2 | 2 | 11 | 1 | 1 | 1 |
| 2 | 3 | 1 | 1 | 3 | 2 | 0 | 2 | 10 | 2 | 2 | 0 | 1 | 3 | 2 | 1 | 2 | 1 | 3 | 3 | 1 | 0 |
| 0 | 0 | 11 | 2 | 0 | 1 | 2 | 0 | 9 | 0 | 2 | 1 | 0 | 3 | 2 | 2 | 1 | 2 | 1 | 3 | 3 | 1 |
| 10 | 0 | 0 | 0 | 9 | 3 | 1 | 3 | 0 | 12 | 2 | 1 | 3 | 0 | 3 | 2 | 0 | 2 | 10 | 2 | 2 | 2 |
| 3 | 11 | 0 | 6 | 10 | 9 | 3 | 1 | 4 | 0 | 1 | 0 | 0 | 2 | 0 | 7 | 9 | 0 | 11 | 2 | 1 | 0 |
| 2 | 0 | 2 | 0 | 1 | 0 | 1 | 0 | 0 | 4 | 6 | 0 | 3 | 0 | 3 | 0 | 1 | 0 | 1 | 0 | 0 | 1 |
| 0 | 1 | 2 | 3 | 11 | 3 | 1 | 2 | 2 | 0 | 1 | 3 | 0 | 2 | 0 | 4 | 0 | 2 | 11 | 1 | 1 | 2 |
| 3 | 2 | 0 | 3 | 0 | 1 | 2 | 3 | 11 | 3 | 1 | 2 | 0 | 1 | 3 | 3 | 0 | 0 | 0 | 6 | 0 | 3 |
| 0 | 2 | 0 | 3 | 0 | 1 | 1 | 0 | 11 | 1 | 2 | 3 | 2 | 2 | 11 | 3 | 0 | 2 | 0 | 4 | 0 | 8 |
| 8 | 0 | 2 | 10 | 2 | 2 | 1 | 4 | 0 | 1 | 0 | 0 | 2 | 0 | 11 | 0 | 6 | 10 | 9 | 0 | 1 | 0 |
| 0 | 0 | 3 | 2 | 0 | 3 | 0 | 3 | 1 | 0 | 2 | 0 | 1 | 0 | 1 | 0 | 0 | 2 | 0 | 1 | 0 | 2 |
| 3 | 1 | 2 | 2 | 0 | 1 | 3 | 0 | 12 | 3 | 3 | 3 | 1 | 0 | 0 | 2 | 10 | 9 | 3 | 1 | 4 | 0 |

Table 14

Traffic flows of 3 bandwidth units for the third sample network

| | | | | | | | | | | | | | | | | | | | | | |
|---|---|---|---|---|---|---|---|---|---|---|---|---|---|---|---|---|---|---|---|---|---|
| 0 | 1 | 2 | 1 | 3 | 1 | 0 | 2 | 2 | 0 | 3 | 2 | 0 | 4 | 0 | 2 | 0 | 0 | 0 | 0 | 2 | 0 |
| 3 | 0 | 0 | 2 | 2 | 2 | 1 | 1 | 1 | 2 | 3 | 0 | 1 | 0 | 3 | 0 | 0 | 2 | 2 | 2 | 1 | 3 |
| 1 | 2 | 0 | 1 | 0 | 2 | 2 | 3 | 1 | 2 | 3 | 0 | 0 | 0 | 1 | 0 | 0 | 1 | 3 | 2 | 1 | 2 |
| 0 | 1 | 0 | 0 | 1 | 3 | 2 | 1 | 2 | 2 | 1 | 2 | 1 | 0 | 0 | 0 | 0 | 1 | 2 | 0 | 0 | 3 |
| 1 | 2 | 0 | 2 | 0 | 1 | 0 | 2 | 0 | 0 | 0 | 0 | 2 | 0 | 0 | 0 | 0 | 2 | 1 | 2 | 0 | 0 |
| 0 | 4 | 1 | 1 | 2 | 0 | 1 | 1 | 3 | 4 | 0 | 1 | 1 | 2 | 1 | 2 | 2 | 3 | 4 | 0 | 1 | 0 |
| 2 | 0 | 0 | 0 | 1 | 2 | 0 | 0 | 3 | 1 | 2 | 0 | 0 | 0 | 0 | 2 | 1 | 2 | 0 | 0 | 2 | 4 |
| 2 | 3 | 2 | 1 | 3 | 4 | 0 | 0 | 0 | 1 | 2 | 0 | 0 | 0 | 0 | 0 | 1 | 2 | 0 | 2 | 1 | 2 |
| 1 | 0 | 0 | 0 | 2 | 1 | 2 | 0 | 0 | 2 | 1 | 3 | 1 | 2 | 3 | 2 | 0 | 0 | 0 | 0 | 2 | 2 |
| 0 | 0 | 0 | 1 | 2 | 0 | 2 | 0 | 3 | 0 | 2 | 0 | 0 | 1 | 2 | 2 | 1 | 1 | 1 | 2 | 3 | 3 |
| 1 | 4 | 0 | 3 | 0 | 0 | 3 | 3 | 0 | 1 | 0 | 1 | 1 | 2 | 3 | 2 | 0 | 4 | 0 | 2 | 0 | 0 |
| 2 | 3 | 2 | 0 | 0 | 0 | 0 | 2 | 2 | 2 | 2 | 0 | 1 | 1 | 0 | 1 | 0 | 2 | 2 | 3 | 1 | 2 |
| 0 | 0 | 1 | 2 | 2 | 3 | 4 | 0 | 1 | 0 | 3 | 0 | 0 | 0 | 2 | 0 | 1 | 0 | 2 | 0 | 0 | 0 |
| 4 | 3 | 0 | 2 | 3 | 3 | 3 | 1 | 0 | 4 | 0 | 1 | 0 | 0 | 0 | 1 | 2 | 0 | 0 | 3 | 1 | 2 |
| 2 | 3 | 2 | 1 | 3 | 4 | 0 | 0 | 0 | 1 | 2 | 2 | 1 | 2 | 0 | 0 | 0 | 0 | 2 | 0 | 0 | 0 |
| 3 | 4 | 0 | 0 | 0 | 1 | 2 | 0 | 0 | 2 | 0 | 1 | 1 | 3 | 4 | 0 | 1 | 1 | 2 | 1 | 2 | 1 |
| 0 | 0 | 1 | 2 | 0 | 0 | 0 | 0 | 0 | 1 | 2 | 0 | 2 | 1 | 4 | 0 | 0 | 0 | 1 | 2 | 0 | 0 |
| 1 | 3 | 2 | 1 | 2 | 2 | 1 | 2 | 1 | 0 | 0 | 0 | 2 | 0 | 2 | 0 | 1 | 0 | 2 | 0 | 0 | 3 |
| 0 | 1 | 1 | 3 | 4 | 0 | 1 | 1 | 2 | 1 | 2 | 2 | 0 | 1 | 1 | 3 | 4 | 0 | 0 | 1 | 2 | 3 |
| 2 | 1 | 2 | 0 | 0 | 2 | 1 | 3 | 1 | 2 | 3 | 0 | 1 | 2 | 0 | 0 | 0 | 0 | 0 | 0 | 1 | 1 |
| 2 | 0 | 0 | 3 | 1 | 2 | 0 | 0 | 0 | 0 | 2 | 4 | 0 | 0 | 0 | 1 | 2 | 0 | 0 | 0 | 0 | 0 |
| 2 | 0 | 0 | 2 | 1 | 3 | 1 | 2 | 3 | 4 | 0 | 0 | 0 | 1 | 2 | 0 | 3 | 3 | 0 | 1 | 0 | 0 |

Table 15

Traffic flows of 12 bandwidth units for the third sample network

| | | | | | | | | | | | | | | | | | | | | | |
|---|---|---|---|---|---|---|---|---|---|---|---|---|---|---|---|---|---|---|---|---|---|
| 0 | 2 | 0 | 3 | 0 | 0 | 2 | 1 | 2 | 0 | 2 | 1 | 0 | 0 | 0 | 3 | 0 | 0 | 2 | 1 | 2 | 0 |
| 0 | 0 | 0 | 1 | 0 | 3 | 2 | 0 | 3 | 0 | 3 | 3 | 1 | 3 | 3 | 0 | 1 | 2 | 0 | 2 | 1 | 1 |
| 0 | 1 | 0 | 0 | 0 | 2 | 3 | 0 | 0 | 3 | 2 | 1 | 0 | 2 | 1 | 0 | 0 | 3 | 1 | 1 | 0 | 2 |
| 1 | 1 | 0 | 0 | 3 | 1 | 1 | 0 | 2 | 0 | 0 | 3 | 1 | 0 | 0 | 2 | 1 | 0 | 0 | 0 | 3 | 0 |
| 3 | 0 | 0 | 2 | 0 | 3 | 0 | 2 | 0 | 2 | 0 | 0 | 0 | 3 | 0 | 2 | 0 | 0 | 1 | 0 | 2 | 0 |
| 1 | 3 | 2 | 0 | 1 | 0 | 2 | 0 | 0 | 1 | 0 | 1 | 0 | 2 | 3 | 2 | 0 | 3 | 0 | 3 | 3 | 1 |
| 1 | 0 | 0 | 0 | 0 | 0 | 0 | 0 | 0 | 3 | 1 | 2 | 2 | 1 | 3 | 2 | 0 | 1 | 0 | 2 | 0 | 0 |
| 0 | 3 | 1 | 0 | 0 | 0 | 0 | 0 | 0 | 0 | 3 | 0 | 0 | 0 | 0 | 1 | 0 | 3 | 2 | 0 | 3 | 0 |
| 0 | 0 | 1 | 2 | 3 | 0 | 1 | 0 | 0 | 2 | 1 | 0 | 0 | 0 | 1 | 2 | 0 | 2 | 1 | 0 | 0 | 0 |
| 0 | 1 | 0 | 1 | 1 | 0 | 0 | 0 | 1 | 0 | 1 | 0 | 0 | 1 | 0 | 3 | 0 | 3 | 3 | 1 | 3 | 3 |
| 1 | 3 | 3 | 0 | 0 | 3 | 1 | 2 | 0 | 0 | 0 | 0 | 1 | 3 | 0 | 0 | 0 | 2 | 3 | 0 | 0 | 3 |
| 1 | 0 | 2 | 2 | 0 | 1 | 0 | 3 | 3 | 3 | 2 | 0 | 3 | 0 | 0 | 3 | 2 | 1 | 0 | 2 | 1 | 0 |
| 0 | 0 | 2 | 3 | 0 | 1 | 2 | 0 | 2 | 1 | 1 | 1 | 0 | 3 | 1 | 3 | 2 | 0 | 1 | 0 | 2 | 0 |
| 0 | 2 | 0 | 0 | 1 | 0 | 2 | 0 | 1 | 0 | 0 | 1 | 0 | 0 | 2 | 1 | 0 | 0 | 0 | 3 | 0 | 0 |
| 0 | 0 | 2 | 1 | 0 | 0 | 0 | 1 | 2 | 0 | 0 | 0 | 2 | 3 | 0 | 0 | 3 | 2 | 0 | 3 | 0 | 2 |
| 0 | 0 | 1 | 2 | 0 | 0 | 3 | 1 | 0 | 0 | 2 | 1 | 0 | 0 | 0 | 0 | 3 | 1 | 2 | 2 | 1 | 0 |
| 0 | 1 | 0 | 1 | 0 | 0 | 1 | 1 | 0 | 0 | 2 | 1 | 0 | 0 | 0 | 1 | 0 | 0 | 0 | 3 | 0 | 0 |
| 0 | 0 | 0 | 1 | 3 | 0 | 0 | 0 | 2 | 3 | 0 | 1 | 2 | 0 | 0 | 0 | 2 | 0 | 3 | 2 | 0 | 3 |
| 0 | 0 | 1 | 0 | 3 | 3 | 3 | 2 | 0 | 3 | 0 | 0 | 3 | 2 | 1 | 0 | 3 | 2 | 0 | 3 | 0 | 3 |
| 0 | 0 | 0 | 1 | 0 | 1 | 0 | 0 | 1 | 0 | 3 | 0 | 3 | 1 | 2 | 0 | 0 | 0 | 2 | 0 | 0 | 0 |
| 3 | 0 | 1 | 3 | 0 | 0 | 0 | 1 | 2 | 2 | 1 | 3 | 2 | 0 | 1 | 0 | 0 | 0 | 3 | 0 | 0 | 3 |
| 3 | 1 | 0 | 0 | 2 | 1 | 0 | 0 | 0 | 0 | 0 | 0 | 0 | 0 | 0 | 3 | 0 | 0 | 0 | 2 | 1 | 0 |

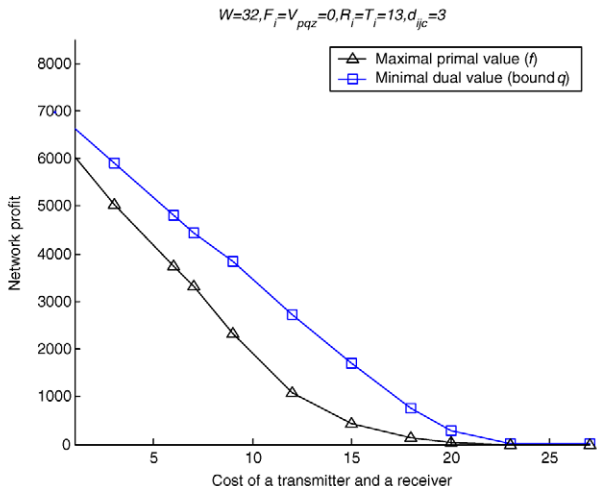


Fig. 10. Profit w.r.t. the transmitter and receiver cost for the third sample network.

Although we have provided a promising framework to solve the profit optimization problem for practical-size networks, the duality gap in some cases is still large. This indicates that the feasible solution is far from the optimal solution. Different heuristics should be investigated to reduce the duality gap. Also Our optimization is so far conducted on individual parameters, more joint optimization using multiple parameters would be desirable.

## Appendix A. Proof of the Eq. (13)

Denote the constraints (4) and (8)–(10) as $h_k(\gamma, \upsilon, \alpha, \delta, \phi) \leqslant 0$ for $k = 1, 2, 3, 4$, respectively. Define the Lagrangian function (12) as $L(\gamma, \upsilon, \alpha, \delta, \phi, \theta, \pi, \xi, \eta)$:

$$L(\gamma, \upsilon, \alpha, \delta, \phi, \theta, \pi, \xi, \eta) = f(\gamma, \upsilon, \alpha, \delta, \phi) + \theta \times h_1(\gamma, \upsilon, \alpha, \delta, \phi) + \pi \times h_2(\gamma, \upsilon, \alpha, \delta, \phi) + \xi \times h_3(\gamma, \upsilon, \alpha, \delta, \phi) + \eta \times h_4(\gamma, \upsilon, \alpha, \delta, \phi). \quad (30)$$

Define the dual function $q(\theta, \pi, \xi, \eta)$ as the supremum of $L$:

$$q(\theta, \pi, \xi, \eta) = \sup_{\gamma,\upsilon,\alpha,\delta,\phi} L(\gamma, \upsilon, \alpha, \delta, \phi, \theta, \pi, \xi, \eta), \quad \theta, \pi, \xi, \eta \leqslant 0. \quad (31)$$

By definition,

$$q(\theta, \pi, \xi, \eta) \geqslant L(\gamma, \upsilon, \alpha, \delta, \phi, \theta, \pi, \xi, \eta). \quad (32)$$

When the dual function reaches its minimum and the Lagrangian function reaches it maximum, the above inequality still holds. Thus,

$$\min_{\theta,\pi,\xi,\eta \leqslant 0} q(\theta, \pi, \xi, \eta) \geqslant \max_{\gamma,\upsilon,\alpha,\delta,\phi} L(\gamma, \upsilon, \alpha, \delta, \phi, \theta, \pi, \xi, \eta). \quad (33)$$

We prove the inequality (13). Considering the non-positive conditions of $\theta, \pi, \xi, \eta$ and $h_k$ for $k = 1, 2, 3, 4$, we derive

$$L(\gamma, \upsilon, \alpha, \delta, \phi, \theta, \pi, \xi, \eta) \geqslant f(\gamma, \upsilon, \alpha, \delta, \phi). \quad (34)$$

Combining the inequalities (32) and (34), we get

$$q(\theta, \pi, \xi, \eta) \geqslant f(\gamma, \upsilon, \alpha, \delta, \phi). \quad (35)$$

So the minimal value of the dual function is an upper bound of the primal function.

$$\min_{\theta,\pi,\xi,\eta \leqslant 0} q(\theta, \pi, \xi, \eta) \geqslant \max_{\gamma,\upsilon,\alpha,\delta,\phi} f(\gamma, \upsilon, \alpha, \delta, \phi). \quad (36)$$

Let us discuss the optimality condition of the problem. We denote $g[f(\gamma, \upsilon, \alpha, \delta, \phi)]$ as the subgradient of $f$. Similarly, we denote $g[h_k(\gamma, \upsilon, \alpha, \delta, \phi)]$ for $k = 1, 2, 3, 4$, as the subgradient of $h_k$. When we ignore the integer constraints for variables $\gamma, \upsilon, \alpha, \delta, \phi$, the Lagrange multiplier theory [21, Chapter 3, Proposition 3.3.6, pp. 327] proves that for the optimal solution $\gamma^*, \upsilon^*, \alpha^*, \delta^*, \phi^*$ of the Lagrangian function (12), there always exist Lagrange multipliers $\theta^*, \pi^*, \xi^*, \eta^*$ that satisfy:

$$g\left[f(\gamma^*, \upsilon^*, \alpha^*, \delta^*, \phi^*)\right] + \theta^* \times g\left[h_1(\gamma^*, \upsilon^*, \alpha^*, \delta^*, \phi^*)\right] + \pi^* \times g\left[h_3(\gamma^*, \upsilon^*, \alpha^*, \delta^*, \phi^*)\right] + \xi^* \times g\left[h_3(\gamma^*, \upsilon^*, \alpha^*, \delta^*, \phi^*)\right] + \eta^* \times g\left[h_4(\gamma^*, \upsilon^*, \alpha^*, \delta^*, \phi^*)\right] = 0. \quad (37)$$

The optimal solution $\gamma^*, \upsilon^*, \alpha^*, \delta^*, \phi^*$ in the optimality condition (37) does not necessarily correspond to the case where all Lagrange multipliers $\theta^*, \pi^*, \xi^*, \eta^*$ are zero. If the Lagrange multipliers $\theta^*, \pi^*, \xi^*, \eta^*$ are zero, and $g[f(\gamma^*, \upsilon^*, \alpha^*, \delta^*, \phi^*)]$ is not zero, then there must exist a solution $\overline{\gamma}, \overline{\upsilon}, \overline{\alpha}, \overline{\delta}, \overline{\phi}$ that satisfies:

$$L(\overline{\gamma}, \overline{\upsilon}, \overline{\alpha}, \overline{\delta}, \overline{\phi}, 0, 0, 0, 0) > L(\gamma^*, \upsilon^*, \alpha^*, \delta^*, \phi^*, 0, 0, 0, 0). \tag{38}$$

This contradicts the assumption that $\gamma^*, \upsilon^*, \alpha^*, \delta^*, \phi^*$ correspond to the maximal value of the Lagrangian function (12). So, when the Lagrange multipliers $\theta^*, \pi^*, \xi^*, \eta^*$ are zero, and $g[f(\gamma^*, \upsilon^*, \alpha^*, \delta^*, \phi^*)]$ is not zero, the Lagrangian function (12) cannot reach its maximal value.

## Appendix B. Manipulation and re-grouping of the Lagrangian function (12)

The Lagrangian function (12) can be re-grouped as:

$$\begin{aligned}
&L(\gamma, \upsilon, \alpha, \delta, \phi, \theta, \pi, \xi, \eta) \\
&\quad = \sum_{(p,q)} \sum_{0<z\leqslant Z_{pq}} \gamma_{pqz} P_{pqz} G_{pqz} - \sum_{(p,q)} \sum_{0<z\leqslant Z_{pq}} E_{pqz} - \sum_{(s,d)} \sum_{0<n\leqslant N_{sd}} D_{sdn} \\
&\qquad + \sum_{(s,d)} \sum_{0<n\leqslant N_{sd}} \theta_{sdn} \Biggl( \sum_{(p,q)} \sum_{0<z\leqslant Z_{pq}} \upsilon_{sdn}^{pqz} G_{pqz} - C\alpha_{sdn} \Biggr) + \sum_{j} \pi_j \Biggl( \sum_{(s,d)} \sum_{0<n\leqslant N_{sd}} \phi_j^{sdn} - F_j \Biggr) \\
&\qquad + \sum_{(i,j)} \sum_{0<c\leqslant W} \xi_{ijc} \Biggl( \sum_{(s,d)} \sum_{0<n\leqslant N_{sd}} \delta_{ijc}^{sdn} - 1 \Biggr) + \sum_{s} \eta_s \Biggl( \sum_{d} \sum_{0<n\leqslant N_{sd}} \alpha_{sdn} - T_s \Biggr) \\
&\quad = -\sum_{(s,d)} \sum_{0<n\leqslant N_{sd}} \theta_{sdn} C\alpha_{sdn} + \sum_{s} \eta_s \sum_{d} \sum_{0<n\leqslant N_{sd}} \alpha_{sdn} - \sum_{(s,d)} \sum_{0<n\leqslant N_{sd}} [\alpha_{sdn}(t_s + r_d)] \\
&\qquad - \sum_{(s,d)} \sum_{0<n\leqslant N_{sd}} \sum_{(i,j)} \sum_{0<c\leqslant W} \delta_{ijc}^{sdn} d_{ijc} + \sum_{(i,j)} \sum_{0<c\leqslant W} \xi_{ijc} \sum_{(s,d)} \sum_{0<n\leqslant N_{sd}} \delta_{ijc}^{sdn} \\
&\qquad - \sum_{(s,d)} \sum_{0<n\leqslant N_{sd}} \sum_{j} \phi_j^{sdn} c_j + \sum_{j} \pi_j \sum_{(s,d)} \sum_{0<n\leqslant N_{sd}} \phi_j^{sdn} + \sum_{(p,q)} \sum_{0<z\leqslant Z_{pq}} \gamma_{pqz} P_{pqz} G_{pqz} \\
&\qquad - \sum_{(p,q)} \sum_{0<z\leqslant Z_{pq}} \sum_{(s,d)} \sum_{0<n\leqslant N_{sd}} \upsilon_{sdn}^{pqz} V_{pqz} + \sum_{(s,d)} \sum_{0<n\leqslant N_{sd}} \theta_{sdn} \sum_{(p,q)} \sum_{0<z\leqslant Z_{pq}} \upsilon_{sdn}^{pqz} G_{pqz} \\
&\qquad - \sum_{j} \pi_j F_j - \sum_{(i,j)} \sum_{0<c\leqslant W} \xi_{ijc} - \sum_{s} \eta_s T_s.
\end{aligned}$$

If lightpath $s_{sdn}$ is not set up, then $s_{sdn}$ does not use any wavelength channels. So, $\alpha_{sdn} = 0$ implies $\delta_{ijc}^{sdn} = 0$ for all wavelength channels $w_{ijc}$. Thus,

$$\alpha_{sdn}\delta_{ijc}^{sdn} = \delta_{ijc}^{sdn} \quad \text{for all lightpaths } s_{sdn} \text{ and all wavelength channels } w_{ijc}. \tag{39}$$

Similarly, if lightpath $s_{sdn}$ is not set up, then $s_{sdn}$ does not use any wavelength converters. So, $\alpha_{sdn} = 0$ implies $\phi_j^{sdn} = 0$ for all intermediate nodes $w_{ijc}$. Thus,

$$\alpha_{sdn}\phi_j^{sdn} = \phi_j^{sdn} \quad \text{for all lightpaths } s_{sdn} \text{ and all intermediate nodes } j. \tag{40}$$

If traffic flow $\chi_{pqz}$ is rejected, then $\chi_{pqz}$ does not use any lightpaths. So, $\gamma_{pqz} = 0$ implies $\upsilon_{sdn}^{pqz} = 0$ for all lightpaths $s_{sdn}$. Thus,

$$\gamma_{pqz}\upsilon_{sdn}^{pqz} = \upsilon_{sdn}^{pqz} \quad \text{for all traffic flows } \chi_{pqz} \text{ and all lightpaths } s_{sdn}. \tag{41}$$

After such manipulations, the Lagrangian function (12) can be re-written as:

$$\begin{aligned}
&L(\gamma,\upsilon,\alpha,\delta,\phi,\theta,\pi,\xi,\eta)\\
&\quad= \Bigg[-\sum_{(s,d)}\sum_{0<n\leqslant N_{sd}}\alpha_{sdn}C\theta_{sdn} + \sum_{(s,d)}\sum_{0<n\leqslant N_{sd}}\alpha_{sdn}\eta_s - \sum_{(s,d)}\sum_{0<n\leqslant N_{sd}}\alpha_{sdn}(t_s + r_d)\\
&\qquad - \sum_{(s,d)}\sum_{0<n\leqslant N_{sd}}\sum_{(i,j)}\sum_{0<c\leqslant W}\alpha_{sdn}\delta_{ijc}^{sdn}d_{ijc} + \sum_{(s,d)}\sum_{0<n\leqslant N_{sd}}\sum_{(i,j)}\sum_{0<c\leqslant W}\alpha_{sdn}\delta_{ijc}^{sdn}\xi_{ijc}\\
&\qquad - \sum_{(s,d)}\sum_{0<n\leqslant N_{sd}}\sum_{j}\alpha_{sdn}\phi_j^{sdn}c_j + \sum_{(s,d)}\sum_{0<n\leqslant N_{sd}}\sum_{j}\alpha_{sdn}\phi_j^{sdn}\pi_j\Bigg]\\
&\qquad + \Bigg(\sum_{(p,q)}\sum_{0<z\leqslant Z_{pq}}\gamma_{pqz}P_{pqz}G_{pqz} - \sum_{(p,q)}\sum_{0<z\leqslant Z_{pq}}\sum_{(s,d)}\sum_{0<n\leqslant N_{sd}}\gamma_{pqz}\upsilon_{sdn}^{pqz}V_{pqz}\\
&\qquad\quad + \sum_{(p,q)}\sum_{0<z\leqslant Z_{pq}}\sum_{(s,d)}\sum_{0<n\leqslant N_{sd}}\gamma_{pqz}\upsilon_{sdn}^{pqz}\theta_{sdn}G_{pqz}\Bigg)\\
&\qquad - \sum_{j}\pi_jF_j - \sum_{(i,j)}\sum_{0<c\leqslant W}\xi_{ijc} - \sum_{s}\eta_sT_s.
\end{aligned}$$

So, the maximization of the Lagrangian function (12) can be written as (14). Note that, the derived Lagrangian function is nonlinear, because it has multiplication of variables.

## References

[1] E. Modiano and P.J. Lin, Traffic grooming in WDM networks, *IEEE Communications Magazine* **39**(7) (2001), 124–129.

[2] R. Dutta and G.N. Rouskas, Traffic grooming in WDM networks: past and future, *IEEE Network* **16**(6) (2002), 46–56.

[3] T. Cinkler, Traffic and $\lambda$ grooming, *IEEE Network* **17**(2) (2003), 16–21.

[4] I. Cerutti and A. Fumagalli, Traffic Grooming in static wavelength division multiplexing networks, *IEEE Communications Magazine* **43**(1) (2005), 101–107.

[5] W. Yao, G. Sahin, M. Li and B. Ramamurthy, Analysis of multi-hop traffic grooming in WDM mesh networks, in: *2nd International Conference on Broadband Networks (BROADNETS 2005)*, IEEE Press, Piscataway, NJ, 2005, pp. 165–174.

[6] R. Ul-Mustafa and A.E. Kamal, Design and provisioning of WDM networks with multicast traffic grooming, *IEEE Journal on Selected Areas in Communications* **24**(Suppl. 4) (2006), 37–53.

[7] J.Q. Hu and B. Leida, Traffic grooming, routing, and wavelength assignment in optical WDM mesh networks, in: *23rd Annual Joint Conference of the IEEE Computer and Communications Societies (INFOCOM 2004)*, IEEE Press, Piscataway, NJ, 2004, pp. 495–501.

[8] K. Zhu and B. Mukherjee, Traffic grooming in an optical WDM mesh network, *IEEE Journal on Selected Areas in Communications* **20**(1) (2002), 122–133.

[9] R. Dutta and G.N. Rouskas, On optimal traffic grooming in WDM rings, *IEEE Journal on Selected Areas in Communications* **20**(1) (2002), 110–121.

[10] C. Xin, B. Wang, X. Cao and J. Li, Logical topology design for dynamic traffic grooming in WDM optical networks, *IEEE/OSA Journal of Lightwave Technology* **24**(6) (2006), 2267–2275.

[11] T. Song, H. Zhang, Y. Guo and X. Zheng, Optimal design of WDM ring networks to minimize SDH ADMs, *Journal of Optical Communications* **24**(3) (2004), 144–148.

[12] A. Chiu and E.H. Modiano, Traffic grooming algorithms for reducing electronic multiplexing costs in WDM ring networks, *IEEE/OSA Journal of Lightwave Technology* **18**(1) (2000), 2–12.

[13] V.R. Konda and T.Y. Chow, Algorithm for traffic grooming in optical networks to minimize the number of transceivers, in: *2001 IEEE Workshop on High Performance Switching and Routing (HPSR 2001)*, IEEE Press, Piscataway, NJ, 2001, pp. 218–221.

[14] D. Zhemin and M. Hamdi, Traffic grooming in optical WDM mesh networks using the blocking island paradigm, *Optical Networks Magazine* **4**(6) (2003), 7–15.

[15] Z. Patrocinio Jr. and G.R. Mateus, A Lagrangian-based heuristic for traffic grooming in WDM optical networks, in: *IEEE Global Telecommunications Conference (GLOBECOM 2003)*, IEEE Press, Piscataway, NJ, 2003, pp. 2767–2771.

[16] Y. Zhang, J. Wu, O. Yang and M. Savoie, A Lagrangian-relaxation based network profit optimization for mesh SONET-over-WDM networks, *Photonic Network Communications* **10**(2) (2005), 155–178.

[17] B. Chen, G.N. Rouskas and R. Dutta, Traffic grooming in WDM ring networks with the min-max objective, in: *3rd International IFIP-TC6 Networking Conference (Networking 2004)*, Lecture Notes in Computer Science, Vol. 3042, Springer-Verlag, Berlin, 2004, pp. 174–185.

[18] M. Sridharan, A.K. Somani and M.V. Salapaka, Approaches for capacity and revenue optimization in survivable WDM networks, *Journal of High Speed Networks* **10**(2) (2001), 109–125.

[19] P. Prathombutr, J. Stach and E.K. Park, An algorithm for traffic grooming in WDM optical mesh networks with multiple objectives, in: *12th International Conference on Computer Communications and Networks (ICCCN 2003)*, IEEE Press, Piscataway, NJ, 2003, pp. 405–411.

[20] D. Palomar and M. Chiang, A tutorial on decomposition methods for network utility maximization, *IEEE Journal on Selected Areas in Communications* **24**(8) (2006), 1439–1451.

[21] D.P. Bertsekas, *Nonlinear Programming*, 2nd edn, Athena Scientific, Belmont, MA, 1999.

[22] I. Chlamtac, A. Farago and T. Zhang, Lightpath (wavelength) routing in large WDM networks, *IEEE Journal on Selected Areas in Communications* **14**(5) (1996), 909–913.

[23] Y. Zhang, O. Yang and H. Liu, A Lagrangian relaxation and subgradient framework for the routing and wavelength assignment problem in WDM networks, *IEEE Journal on Selected Areas in Communications* **22**(9) (2004), 1752–1765.